Article

Molecular Cell

# PELI1 Selectively Targets Kinase-Active RIP3 for Ubiquitylation-Dependent Proteasomal Degradation

## Graphical Abstract

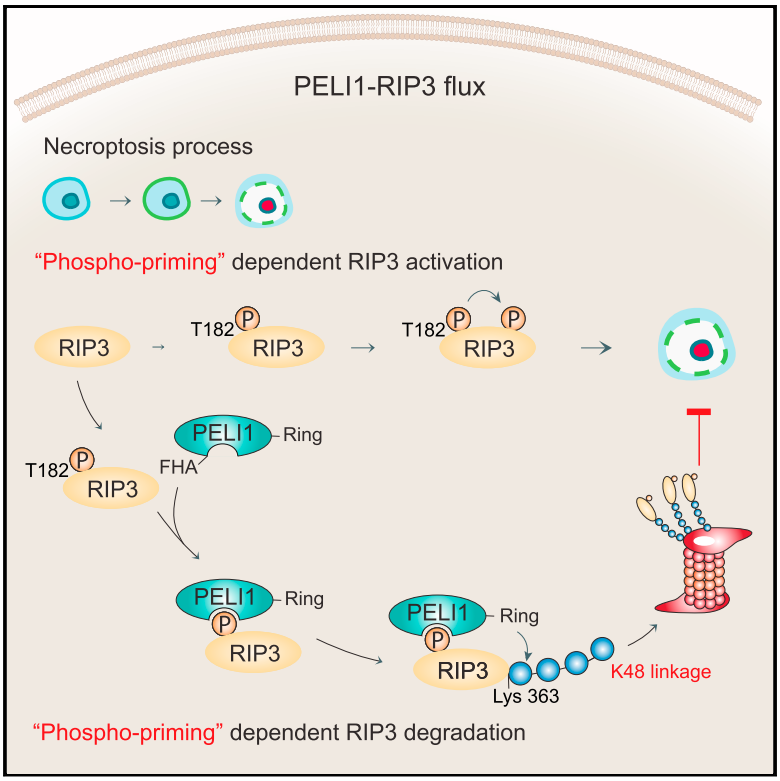


## Authors

Seung-Won Choi, Han-Hee Park, Soyeon Kim, ..., Michael J. Morgan, Ho Chul Kang, You-Sun Kim

## Correspondence

hckang@ajou.ac.kr (H.C.K.), yousunkim@ajou.ac.kr (Y.-S.K.)

## In Brief

Choi et al. show that PELI1-mediated K48-linked polyubiquitylation of kinase-active RIP3 leads to its proteasome-dependent degradation. Regulation of activated RIP3 by PELI1 provides a homeostatic mechanism to prevent aberrant cell death and minimize necroptotic pathology that occurs in diseases such as toxic epidermal necrolysis.

## Highlights

- Active RIP3 kinase interacts directly with PELI1 through its FHA domain
- Polyubiquitylation of RIP3 (K363) by PELI1 leads to proteasome-dependent degradation
- RIP3 phosphorylation at T182 is necessary for kinase activity and PELI1 recruitment
- PELI1 may block inadvertent activation of RIP3, thus preventing aberrant cell death

Choi et al., 2018, Molecular Cell *70*, 920–935
June 7, 2018 
https://doi.org/10.1016/j.molcel.2018.05.016

CellPress

CellPress

Molecular Cell
Article

# PELI1 Selectively Targets Kinase-Active RIP3 for Ubiquitylation-Dependent Proteasomal Degradation

Seung-Won Choi,[1,2,9] Han-Hee Park,[1,3,9] Soyeon Kim,[4] Jee Min Chung,[4] Hyun-Jin Noh,[1,3] Sue Kyung Kim,[5] Hyun Kyu Song,[6] Chang-Woo Lee,[7] Michael J. Morgan,[8] Ho Chul Kang,[2,4,*] and You-Sun Kim[1,2,3,10,*]
[1]Department of Biochemistry, Ajou University School of Medicine, Suwon, Korea
[2]Genomic Instability Research Center, Ajou University, School of Medicine, Suwon, Korea
[3]Department of Biomedical Sciences, Graduate School, Ajou University, Suwon, Korea
[4]Department of Physiology, Ajou University School of Medicine, Suwon, Korea
[5]Department of Dermatology, Ajou University, School of Medicine, Suwon, Korea
[6]Department of Life Sciences, Korea University, Seoul, Korea
[7]Department of Molecular Cell Biology, Sungkyunkwan University School of Medicine, Suwon, Korea
[8]Department of Pharmacology, University of Colorado School of Medicine, Aurora, CO, USA
[9]These authors contributed equally
[10]Lead Contact
*Correspondence: hckang@ajou.ac.kr (H.C.K.), yousunkim@ajou.ac.kr (Y.-S.K.)
https://doi.org/10.1016/j.molcel.2018.05.016

## SUMMARY

**Receptor-interacting protein kinase-3 (RIP3 or RIPK3) is a central protein in necroptosis, but post-translational processes that regulate RIP3 activity and stability remain poorly understood. Here, we identify pellino E3 ubiquitin protein ligase 1 (PELI1) as an E3 ligase that targets RIP3 for proteasome-dependent degradation. Phosphorylation of RIP3 on T182 leads to interaction with the forkhead-associated (FHA) domain of PELI1 and PELI1-mediated K48-linked polyubiquitylation of RIP3 on K363. This same phosphorylation event is also important for RIP3 kinase activity; thus, PELI1 preferentially targets kinase-active RIP3 for degradation. PELI1-mediated RIP3 degradation effectively prevents cell death triggered by RIP3 hyperactivation. Importantly, upregulated RIP3 expression in keratinocytes from toxic epidermal necrolysis (TEN) patients is correlated with low expression of PELI1, suggesting that loss of PELI1 may play a role in the pathogenesis of TEN. We propose that PELI1 may function to control inadvertent activation of RIP3, thus preventing aberrant cell death and maintaining cellular homeostasis.**

## INTRODUCTION

Necroptosis is distinguished from apoptosis in that it does not require caspases, and unlike apoptosis, necroptosis directly results in plasma membrane rupture (Cho et al., 2009; He et al., 2009; Mocarski et al., 2011; Morgan and Liu, 2013; Vandenabeele et al., 2010). Repression of necroptosis by apoptotic proteins is essential for proper mammalian development (Kaiser et al., 2011; Vanden Berghe et al., 2014) and prevents spontaneous cell death and inflammation (Bonnet et al., 2011; Günther et al., 2011; Mocarski et al., 2014; Welz et al., 2011), underscoring the physiological relevance of necroptosis. In cancer, necroptosis is more efficient at engaging anti-tumor immunity than either apoptosis or accidental necrosis (Aaes et al., 2016; Yatim et al., 2015) and therefore may contribute to tumor suppression. Receptor-interacting protein kinase-3 (RIP3, or RIPK3) is an essential protein for necroptosis, along with its upstream sister kinase RIP1, which it interacts with via a homotypic interaction motif (RHIM) (Li et al., 2012). Mixed-lineage kinase domain-like protein (MLKL) is an essential target of RIP3 kinase activity in necroptosis (Cai et al., 2014; Chen et al., 2014; Li et al., 2012; Wang et al., 2014) that is induced by such stimuli as tumor necrosis factor alpha (TNF-α), Fas ligand, lipopolysaccharide (LPS), T cell receptor (TCR) ligands, and double stranded RNA (Vanlangenakker et al., 2012).

Some reports indicate that RIP3 is regulated by post-translational modification (Chen et al., 2015; He et al., 2009; Koo et al., 2015; Morgan and Kim, 2015; Onizawa et al., 2015; Seo et al., 2016). Protein phosphatase 1B (Ppm1b) was identified as a RIP3 phosphatase that protects from TNF-α-induced necroptosis or RIP3-drivened spontaneous necroptosis by dephosphorylation of S227 (Chen et al., 2015). Deubiquitylating enzyme A20 can reverse Lys 5 RIP3 ubiquitylation, which promotes necrosome assembly and necroptosis (Onizawa et al., 2015). Recently, the C terminus of Hsp-70-interacting protein (CHIP) was shown to mediate ubiquitylation- and lysosome-dependent RIP3 degradation, consequently leading to the regulation of necroptosis (Seo et al., 2016).

Here, we identify the pellino E3 ubiquitin protein ligase 1 (PELI1) as a RIP3 binding partner in proteome microarrays. PELI1 binds to kinase-proficient RIP3 through its forkhead-associated

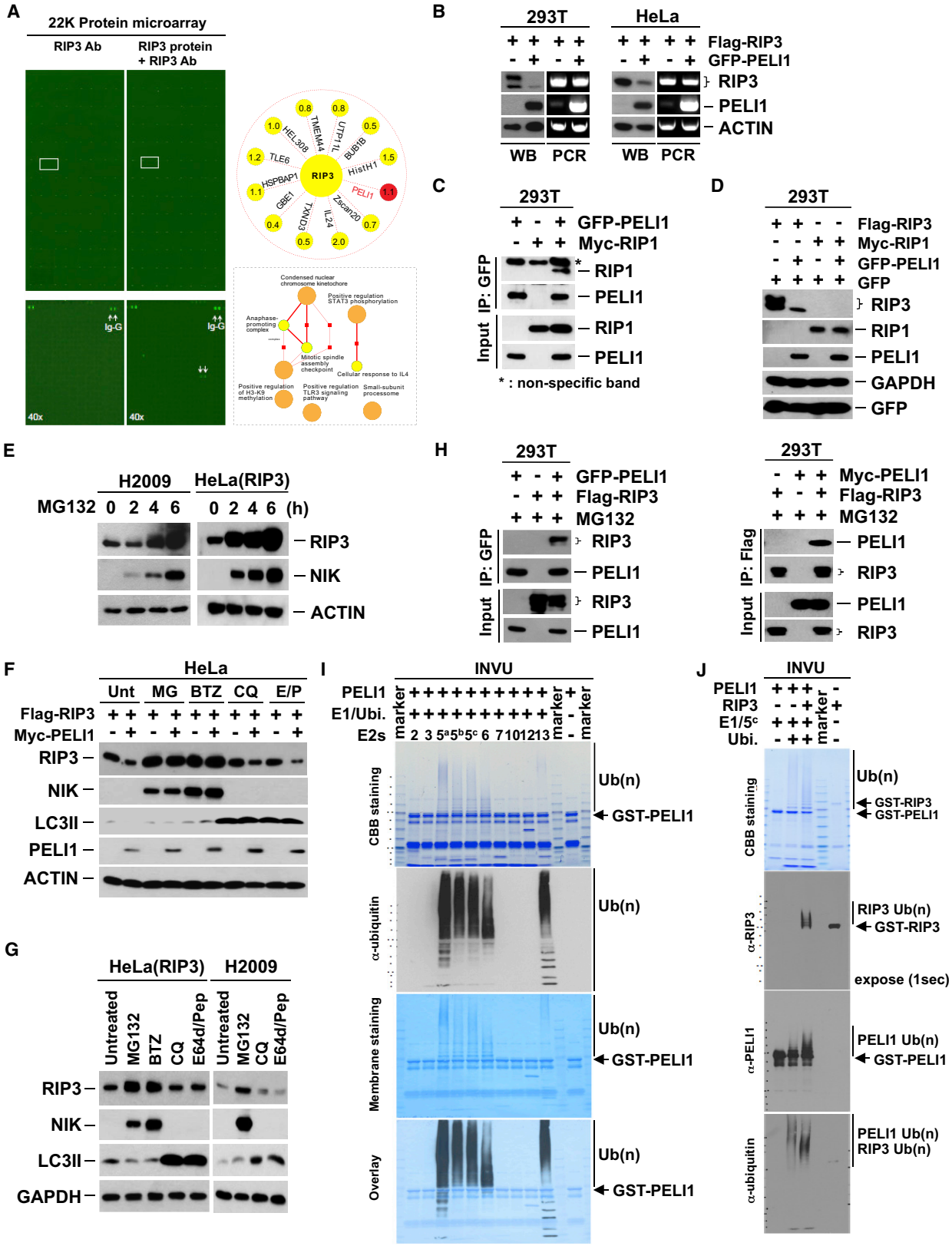


*(legend on next page)*

(FHA) domain and promotes K48-linked polyubiquitylation of RIP3 on lysine 363, leading to RIP3 proteasomal degradation. Disruption of a phosphothreonine (pT) motif within the active loop of RIP3 blocks recognition by PELI1 and prevents RIP3 ubiquitylation and degradation as well as TNF-induced necroptosis. Mouse embryonic fibroblast (MEFs) lacking PELI1 have increased RIP3 and MLKL phosphorylation, and necroptosis in response to necroptotic stimuli. In keratinocytes from toxic epidermal necrolysis (TEN) patients, PELI1 expression is low and inversely correlated with RIP3 protein, suggesting that reduction in PELI1 leads to upregulated RIP3 expression, thus contributing to disease progression. Our results reveal a new mechanism for post-translational modification of RIP3 by PELI1 and subsequent downregulation of necroptosis; this provides a homeostatic mechanism to prevent aberrant cell death and inflammation.

## RESULTS

### PELI1 Is a Novel Binding Partner of RIP3

To identify RIP3-interacting proteins, recombinant RIP3 protein was applied on HuProt v2.0 human proteome microarrays (V2.0, CDI Laboratories) containing 19,000 unique purified human proteins. We identified 12 proteins as direct RIP3-interacting proteins (Figure 1A). Of these, only 6 proteins had a signal-to-noise ratio (SNR) above 1.0: among these was pellino E3 ubiquitin protein ligase 1 (PELI1) (Figure 1A). Co-expression of PELI1 with RIP3 decreased RIP3 expression but did not alter RIP3 mRNA expression (Figure 1B). In contrast, another candidate protein from our screen, BUB1B, interacted with RIP3 but did not affect RIP3 protein levels (Figure S1A). Expression of PELI1 did not affect RIP3 solubility (Figure S1B).

RIP1, which is upstream of RIP3, has been reported to be a substrate of PELI1 (Chang et al., 2009). RIP1 interacted with PELI1 in 293T cells, but unlike RIP3, PELI1 expression did not affect RIP1 protein expression (Figures 1C and 1D), suggesting that PELI1 mediates different effects on the sister kinases. Importantly, PELI1 reduced endogenous RIP3 in H2009 and Raji cell lines (Figure S1C); conversely, knockdown of PELI1 in HT-29 and RIP3 (ectopic)-expressing HeLa cell lines led to increased RIP3 protein without affecting RIP3 mRNA expression (Figure S1D).

### PELI1 Causes Proteasome-Dependent Degradation of RIP3

As PELI1 is an E3 ubiquitin ligase, we explored whether PELI1 regulated RIP3 protein stability through ubiquitylation. Like NIK, which is constitutively degraded by the proteasome, inhibition of proteasome function by MG132 led to increased RIP3 protein (Figure 1E). A recent study concluded that RIP3 was lysosomally degraded after modification by the CHIP E3 ubiquitin ligase (Seo et al., 2016). PELI1-facilitated RIP3 degradation was prevented by proteasome inhibitors (MG132 and BTZ), but not by lysosome inhibitors (CQ and E64d/Pep A) (Figure 1F). Importantly, stably expressed and endogenous RIP3 protein accumulated upon proteasome inhibition, but minimal increase was seen under lysosome inhibition (Figures 1G and S1E). A substantial increase in the half-life of endogenous RIP3 was observed in PELI1-depleted H2009 cells (Figure S1F), indicating that PELI1 controls steady-state levels of RIP3. Proteasome inhibition potentiated the interaction between PELI1 and RIP3 (Figure 1H).

We next screened ubiquitin-conjugating enzymes (E2s) for PELI1's E3 ubiquitin ligase activity using an *in vitro* ubiquitylation assay, which showed that PELI1 utilized the E2s UbcH5a, 5b, 5c, 6, and 13, but not UbcH2, 3, 7, 10, and 12 (Figure 1I). When UbcH5c was provided with recombinant RIP3 and PELI1, RIP3 was drastically ubiquitylated by PELI1 *in vitro* (Figure 1J). TRAF2, an E3 ubiquitin ligase that regulates NIK stabilization (Gardam et al., 2008; Grech et al., 2004; Yang and Sun, 2015), had no effect on RIP3 protein stability, indicating that RIP3 is a specific substrate of PELI1 (Figure S1G). Thus, PELI1 controls RIP3 protein destabilization via ubiquitylation-dependent proteasome-mediated degradation.

### PELI1 Mediates K48-Linked RIP3 Polyubiquitylation

Proteasome inhibition not only increased RIP3 protein in cells but also allowed detection of ubiquitylated RIP3, which was not

**Figure 1. The E3 Ubiquitin Ligase PELI1 Is a Novel Binding Partner of RIP3**

(A) Representative protein chips treated with RIP3 antibody are shown in the presence/absence of recombinant RIP3 (left upper panels), with a magnification of PELI1 binding (white square boxes) shown in the bottom left. RIP3-interacting proteins are shown in the right panel.

(B) 293T cells were transfected with FLAG-RIP3 in the absence/presence of GFP-tagged PELI1 (left panel). GFP-PELI1 was transfected into RIP3 (stable ectopic)-expressing HeLa cells (right panel). After 24 hr, protein/mRNA expression was examined by western blotting/RT-PCR of lysates.

(C) 293T cells were transfected with GFP-PELI1 and/or Myc-RIP1 expression constructs. After 24 hr, cells were harvested and GFP immunoprecipitated. Immunoprecipitates and total lysates were analyzed by western blotting.

(D) 293T cells were transfected with FLAG-RIP3 or Myc-RIP1 with or without GFP-PELI1. The cells were harvested after 24 hr, and cell lysates analyzed by western blotting.

(E) H2009 cells (left panel) or RIP3-expressing HeLa cells (right panel) were treated with 10 μM MG132, and cell lysates were analyzed by western blotting.

(F) HeLa cells were transfected with FLAG-RIP3 with or without Myc-PELI1 in the absence or presence of inhibitors (5 nM bortezomib [BTZ] for 12 hr, 10 μM MG132, 50 μM CQ, or 10 μg/mL E64d plus 10 μg/mL pepstatin for 6 hr). Cell lysates were analyzed by western blotting. NIK and LC3II blots serve as controls for blocking proteasome- and lysosome-dependent degradation, respectively.

(G) RIP3-expressing HeLa cells (left panel) or H2009 cells (right panel) were treated with inhibitors. Cell lysates were analyzed by western blotting.

(H) FLAG-RIP3 and/or GFP-PELI1 (left panel) or FLAG-RIP3 and/or Myc-PELI1 were transfected into 293T cells. After 20 hr, including 10 μM MG132 for the final 3 hr, lysates were immunoprecipitated with GFP or FLAG antibodies.

(I) An *in vitro* ubiquitylation assay was performed with the indicated E2 enzymes, and samples were subjected to immunoblot assay with anti-ubiquitin antibody.

(J) *In vitro* ubiquitylation assays with recombinant PELI1, RIP3, and UbcH5c. RIP3 ubiquitylation was monitored with anti-ubiquitin or anti-RIP3 antibodies. PELI1 E3 ligase activity was monitored with anti-PELI1 antibody. Data are representative of at least three independent experiments.

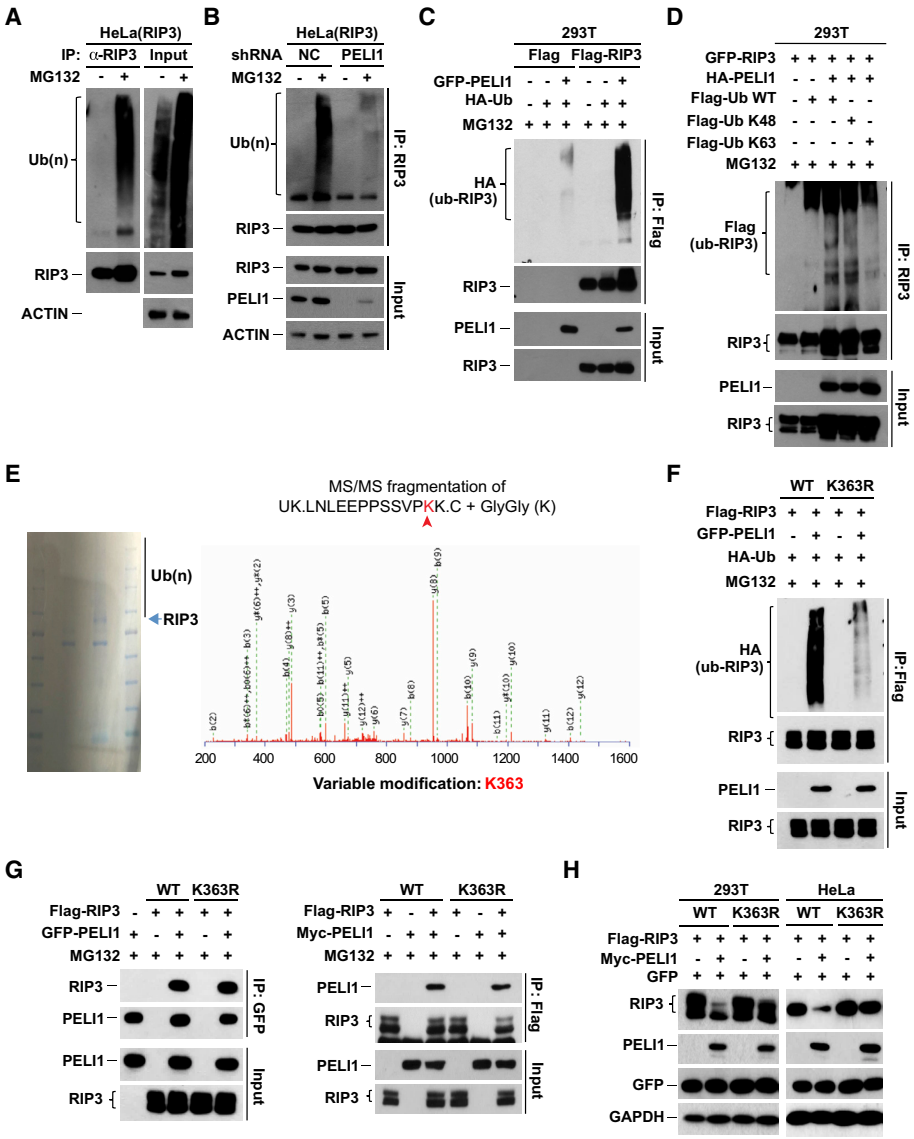


**Figure 2. PELI1 Mediates K48-Linked Polyubiquitylation of RIP3**

(A) RIP3-expressing HeLa cells were treated with DMSO or 10 μM MG132. After 6 hr, lysates were immunoprecipitated with an anti-RIP3 antibody. Ubiquitylation of RIP3 was analyzed by western blotting.

(B) RIP3-expressing HeLa cells were infected with shRNA lentivirus (control or PELI1) for 46 hr. For the final 6 hr, 10 μM MG132 was included where indicated. Anti-RIP3 immunoprecipitates and total lysates were analyzed by western blotting.

(C) 293T cells were transfected with FLAG-RIP3 or empty vector with/without HA-Ub in the absence/presence of GFP-PELI1. At 20 hr after transfection, which included a final 3 hr of 10 μM MG132 incubation, cell lysates were immunoprecipitated with an anti-FLAG antibody.

(D) HA-PELI1 and/or GFP-RIP3 were transfected into 293T cells in the absence or presence of FLAG-tagged wild-type Ub, K48 Ub, or K63 Ub for 20 hr. Transfected cells were exposed to 10 μM MG132 for the final 3 hr of incubation. Cell lysates were immunoprecipitated with an anti-RIP3 antibody.

(E) Ubiquitylated RIP3 was purified by in-gel digestion, and the ubiquitylation site of RIP3 was identified using liquid chromatography-tandem mass spectrometry (LC-MS/MS) analysis.

(F) FLAG-RIP3 WT or a FLAG-RIP3 K363R mutant were transfected into 293T cells in the presence of HA-Ub with or without GFP-PELI1 expression. After 20 hr of transfection, which included a final 3 hr of 10 μM MG132 incubation, cell lysates were immunoprecipitated with an anti-FLAG antibody.

(G) 293T cells were transfected with FLAG-tagged WT or K363R RIP3 in the absence or presence of GFP-PELI1 or Myc-PELI1 for 20 hr. Transfected cells exposed to 10 μM MG132 for the final 3 hr of transfection. Anti-GFP (left panel) or anti-FLAG (right panel) antibodies were applied for immunoprecipitation.

(H) FLAG-tagged WT or K363R RIP3 were transfected into 293T cells in the absence or presence of Myc-PELI1. After 24 hr of transfection, the cell lysates were analyzed by western blotting (left panel). HeLa cells were transfected with FLAG-tagged WT or K363R RIP3 with or without Myc-PELI1. After 36 hr of transfection, cell lysates were analyzed by western blotting (right panel). The plasmid expressing GFP was used as a transfection control.

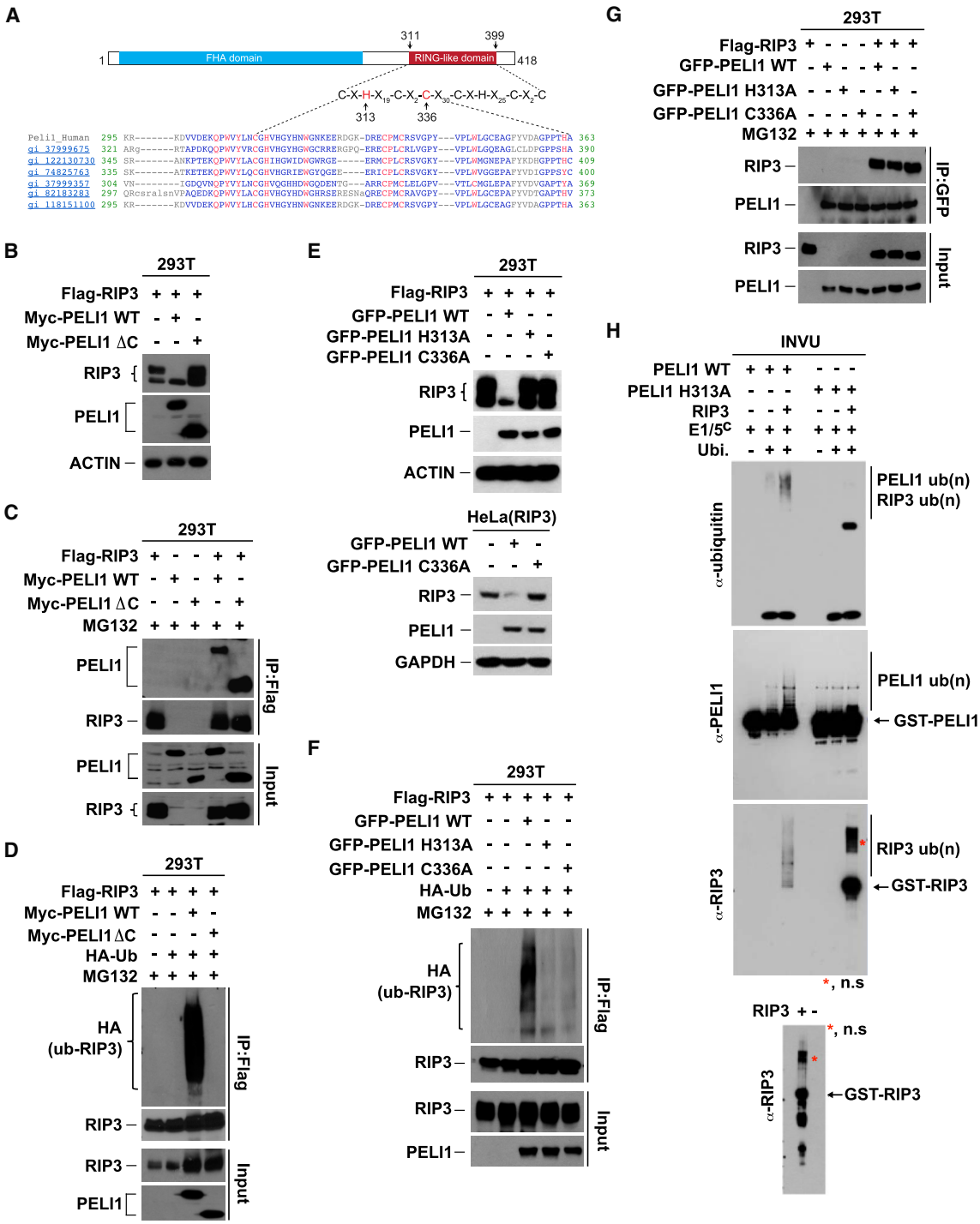


**Figure 3. The RING-like Domain of PELI1 Is Necessary for RIP3 Ubiquitylation and Degradation**

(A) Protein-sequence-based schematic representation of the conserved RING-like domain of PELI1 from several species.

(B) FLAG-RIP3 was transfected into 293T cells in the absence or presence of Myc-tagged WT or ΔC PELI1 for 24 hr. Cell lysates were analyzed by western blotting.

(C) 293T cells were transfected with FLAG-RIP3 in the absence or presence of Myc-tagged WT or ΔC PELI1for 20 hr. Transfected cells were exposed to 10 μM MG132 for the final 3 hr of transfection. Cell lysates were immunoprecipitated with an anti-FLAG antibody.

(D) FLAG-RIP3 and/or HA-Ub was transfected into 293T cells in the absence or presence of Myc-tagged WT or ΔC PELI1. At 16 hr after transfection, cells were treated with 10 μM MG132 for 3 hr and harvested for immunoprecipitation with an anti-FLAG antibody.

*(legend continued on next page)*

observed otherwise (Figure 2A). RIP3 ubiquitylation was eliminated when endogenous PELI1 was depleted by short hairpin RNA (shRNA) (Figure 2B); transient expression of PELI1 promoted ubiquitylation of co-expressed RIP3 (Figures 2C and S2A–S2C). The E3 ligase TRAF2, which also interacts with RIP3, did not affect RIP3 ubiquitylation (Figures S2D and S2E).

Ubiquitin has seven lysine residues available to modify proteins through different linkages. Lys48- and Lys63-linked chains are the best understood modifications in modulating protein degradation and signal transduction, respectively (Ye and Rape, 2009). Using ubiquitin expression constructs where all lysines except these are mutated to arginine indicated that K48-only, but not K63-only, ubiquitin, allowed RIP3 ubiquitylation to occur (Figures 2D and S2F). Conversely, RIP1 could be ubiquitylated by PELI1 via K63-linked, but not K48-linked, chains (Figure S2G), as reported previously (Chang et al., 2009). These results suggest that PELI1 interacts with both RIP1 and RIP3 but modifies them differently.

We identified RIP3 K363 as the main target for PELI1-mediated ubiquitylation by mass spectrometric analysis (Figure 2E). This is one of several RIP3 lysines (K55, K89, K363, and K501) reported to be modified by CHIP (Seo et al., 2016). We generated several RIP3 mutants, including K363R, K501R, and K5R, which are reported ubiquitinylated sites (Onizawa et al., 2015; Seo et al., 2016), as well as K259R and K351R, which are predicted (UbPred: www.ubpred.org). Among these, only the K363R mutation abolished ubiquitylation by PELI1 and prevented PELI1-mediated degradation (Figures 2F, S2H, and S2I), consistent with the mass spectrometric data. While PELI1 was unable to ubiquitylate K363R-RIP3, this mutant maintained its interaction with PELI1 (Figure 2G), but PELI1 did not affect its stability (Figure 2H). These results indicate that PELI1 induces K48-linked RIP3 polyubiquitylation on lysine 363.

## The PELI1 RING-like Domain Is Required for RIP3 Ubiquitylation and Degradation

The RING-like domain in PELI1 is necessary for its E3 ubiquitin ligase activity (Chang et al., 2011; Ordureau et al., 2008; Park et al., 2014; Xiao et al., 2013). C-terminal deletion of this domain (amino acids 1–280; Myc-PELI1 ΔC) (Figure 3A) eliminated RIP3 degradation (Figure 3B). Though both wild-type (WT) and ΔC proteins interacted with RIP3 (Figure 3C), the ΔC mutant could not ubiquitylate RIP3 (Figure 3D), indicating an important role for the RING-like domain in this process. Conserved cysteine and histidine residues ($C_3HC_4$) buried within PELI1's RING-like domain maintain overall structure through coordinating zinc cations (Borden and Freemont, 1996; Deshaies and Joazeiro, 2009). E3-ligase-activity-defective mutants PELI1-H313A or PELI1-C336A (Figure 3A) could not cause RIP3 degradation (Figure 3E) or ubiquitylate RIP3 (Figures 3F and 3H) but, like the PELI1 ΔC mutant, maintained their interaction with RIP3 (Figure 3G). These results demonstrate that the RING-like domain of PELI1 is required for RIP3 ubiquitylation and degradation but dispensable for RIP3 interaction.

## The PELI1 FHA Domain Mediates Its Interaction with RIP3

The PELI1 FHA domain mutant R104A is defective in substrate recognition (Figure 4A) and prevents interaction with IRAK1 (Figure 4B), a known PELI1 target (Huoh and Ferguson, 2014). RIP3 degradation by PELI1 R104A was attenuated (Figure 4C); the R104A mutant failed to interact with both RIP3 and RIP1 (Figure 4D) and largely lost the ability to mediate RIP3 ubiquitylation (Figure 4E). Thus, the FHA domain of PELI1 is important for RIP3 recognition.

FHA domains bind to pT motifs, with the third amino acid following pT also being important for binding (Durocher et al., 1999, 2000; Huoh and Ferguson, 2014; Li et al., 2000, Lin et al., 2008). RIP3 contains 7 putative pT motifs (Figure 4A); alanine mutation of T182 protected RIP3 from degradation by PELI1, whereas T200A, T224A, T300A, T325A, T369A, and T387A mutants were degraded (Figure 4F, in 293T; Figure 4G, in HeLa). The RIP3 T182A mutant failed to interact with (Figure 4H) and be ubiquitylated by PELI1 (Figure 4I). Pellino FHA recognition sequences are known to recognize pTxxD, pTxxI, pTxxY, and pTxxS motifs (Durocher et al., 1999; Huoh and Ferguson, 2014; Li et al., 2000). RIP3 Y185A and Y185F mutants, like the RIP3 T182A mutant, failed to interact with PELI1 (Figure S3A) and were protected from PELI1-mediated degradation (Figure S3B). These data suggest that T182 and Y185 are part of a canonical PELI1 FHA binding motif in RIP3.

## A Lower-Mobility Phospho-RIP3 Species Is Preferentially Recognized by PELI1

Upon overexpression in 293T cells, two RIP3 bands were detected; the upper band disappeared upon phosphatase treatment (Figure S4A), indicating the upper band represents a phosphorylated species of RIP3. The ratio of the upper band to the lower band noticeably increased with the amount of RIP3 overexpression (Figure S4B), perhaps indicating that the phospho-band was the result of RIP3-dependent, self-directed kinase activity activated by its overexpression. While both

(E) FLAG-RIP3 was transfected into 293T cells with GFP-tagged WT, H313A, or C336A PELI1. At 24 hr post-transfection, cell lysates were analyzed by western blotting (upper panel). RIP3-expressing HeLa cells were transfected with GFP-tagged WT or C336A PELI1. After 36 hr of transfection, cell lysates were analyzed by western blotting (lower panel).

(F) FLAG-RIP3 and/or HA-Ub were transfected into 293T cells in the absence or presence of GFP-tagged WT, H313A or C336A PELI1 for 20 hr. Transfected cells were treated with 10 μM MG132 for the final 3 hr of incubation. Cell lysates were immunoprecipitated with an anti-FLAG antibody.

(G) 293T cells were transfected with FLAG-RIP3 in the absence or presence of GFP-tagged WT, H313A, or C336A PELI1 for 20 hr. Transfected cells were treated with 10 μM MG132 for the final 3 hr of transfection, and cell lysates were immunoprecipitated with an anti-GFP antibody.

(H) *In vitro* ubiquitylation assay was performed with His-ubiquitin, GST-E1, Ubc-H5c, RIP3, and recombinant PELI1 WT, H313A mutants purified from insect cells as indicated.

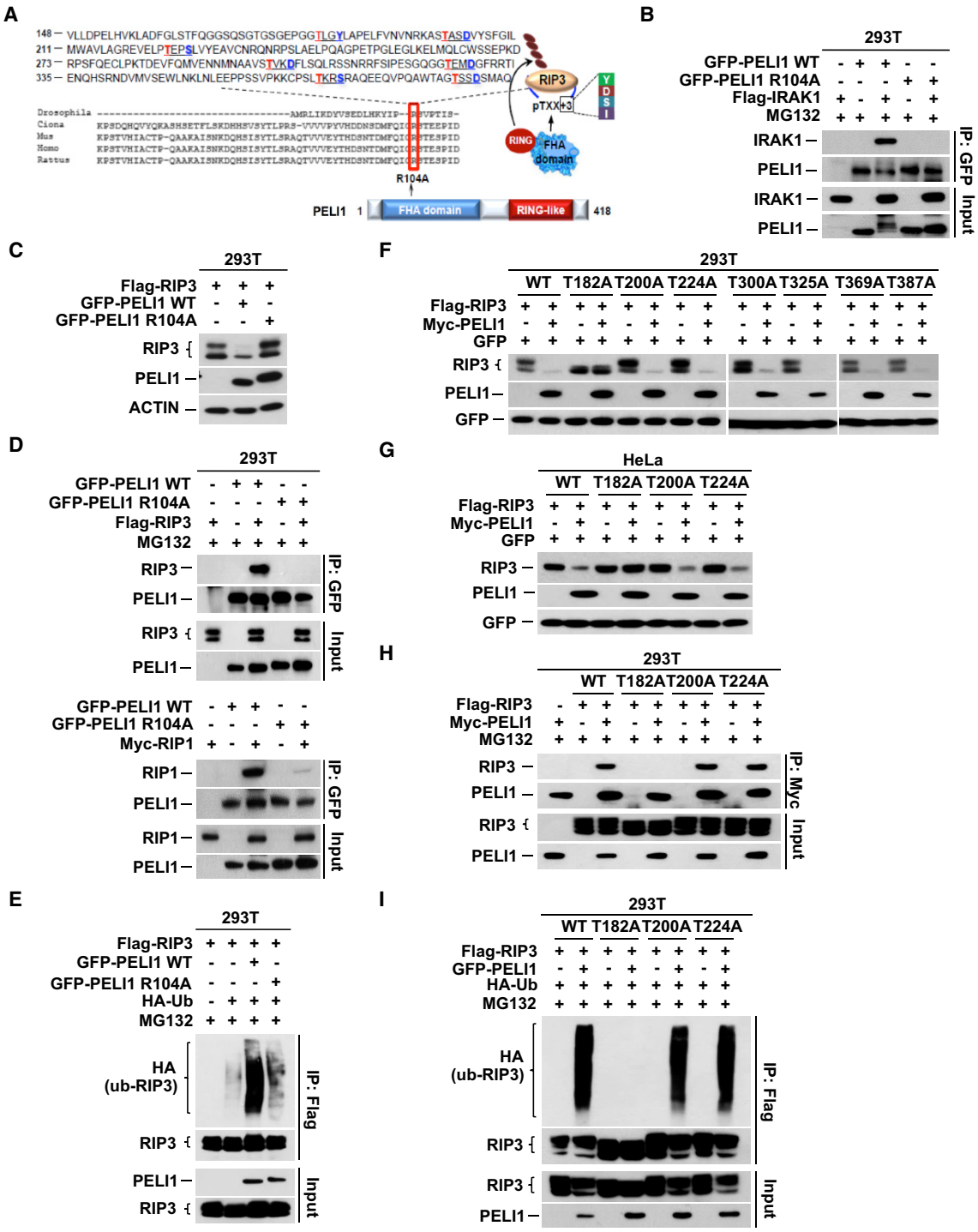


**Figure 4. Arginine 104 in the FHA Domain of PELI1 Is Important for Substrate Recognition**

(A) Schematic representation of PELI1 forkhead-associated (FHA) domain and putative recognition motifs in RIP3 recognized by PELI1.

(B) GFP-tagged WT or R104A PELI1 was transfected into 293T cells with or without FLAG-IRAK1. After 20 hr of transfection, which included a final 3 hr of 10 μM MG132 treatment, cell lysates were immunoprecipitated with a GFP antibody.

(C) 293T cells were transfected with FLAG-RIP3 in the absence or presence of GFP-tagged WT or R104A PELI1 for 24 hr. Cell lysates were analyzed by western blotting.

(D) 293T cells were transfected with GFP-tagged WT or R104A PELI1 in the presence or absence of FLAG-RIP3 (top panel) or Myc-RIP1 (bottom panel). After 20 hr, which included 10 μM MG132 for the final 3 hr, cell lysates were immunoprecipitated with an anti-GFP antibody.

*(legend continued on next page)*

bands of RIP3 were degraded by PELI1, the upper band was degraded to a greater extent than the lower band (see Figure 4C, for instance). Co-immunoprecipitation assays revealed that PELI1 interacts strongly with the upper RIP3 band but weakly with the lower band (Figure S4C). When examining our previous data, we noticed that T182A RIP3 lacked this upper band associated with preferential PELI1 interaction (Figure 4F), consistent with its inability to interact with and be ubiquitylated by PELI1. Thus, it is likely that this upper band either represents phospho-T182 RIP3 itself or another phosphorylated form of RIP3 that is dependent on T182 phosphorylation for priming.

We next compared the ability of CHIP and PELI1 to interact with and ubiquitylate T182A RIP3. Ubiquitylation of T182A RIP3 by PELI1 was substantially reduced; however, both RIP3 WT and T182A mutant were equally ubiquitylated by CHIP (Figure 5A). Consistent with this ability, CHIP interacted with both RIP3 WT and its T182A mutant equally (Figure 5B) and caused the degradation of both WT and T182A RIP3 (Figure 5C). Thus, though both CHIP and PELI1 interact with and ubiquitylate RIP3, they recognize RIP3 differently.

## RIP3 Kinase Activity Is Required for Its Interaction with PELI1, but Not CHIP

Unlike the RIP3 T182A mutant, the T182S mutant bound to PELI1 (Figure 5D), and could be degraded (Figure 5E) and ubiquitylated (Figure 5F) by it, suggesting that phosphoserine can substitute for pT in the FHA recognition motif. Kinases are often activated by auto-phosphorylation of activation loop residues, which then counteracts a positive charge of the arginine in the catalytic loop His-Arg-Asp (HRD) motif. A model of the human RIP3 kinase domain that we generated based on the mouse RIP3 structure (Xie et al., 2013) indicated that T182 is located within the activation loop and is close to D142 in the HRD motif; it is also close to D160 in the tripeptide Asp-Phe-Gly, which interacts with the γ-phosphate of ATP (Figure 5G). This suggests that Thr182 is a likely auto-phosphorylation target and may be involved in RIP3 activity.

To verify T182 phosphorylation, we generated a phospho-T182 antibody. In HT-29 cells, (in which a small amount of basal RIP3 activation is detected by phospho-S227 and MLKL phosphorylation; e.g., Figure 7), we could detect phospho-T182 upon high exposure of the immunoblot; this band diminished with RIP3 knockdown (Figure 5H). Phosphorylation of T182 was also detected upon overexpression of RIP3 WT in 293T cells; this band was absent when the RIP3 T182A mutant was overexpressed (Figure 5I). Interestingly, while phospho-S227 was also detected upon overexpression of WT RIP3, it was also not observed upon T182A mutant overexpression (Figure 5I). The T182A mutant was the only threonine mutant that we tested that lacked phosphorylation of S227 upon overexpression (Figure S4D), which may suggest that phospho-Thr182 is important for RIP3 kinase activity in addition to its being part of the recognition motif bound by the FHA domain of PELI1.

We therefore examined whether RIP3 kinase activity was important for PELI1-mediated RIP3 degradation. Phosphorylation of Ser-227, which is required for downstream MLKL activation, was not required for PELI1-mediated degradation, as S227A and S227D mutations did not affect degradation by PELI1 (Figure S4E). Inhibition of RIP3 kinase activity by dabrafenib (Li et al., 2014), however, completely abolished PELI1-mediated RIP3 degradation (Figures 5J and S4F). Furthermore, a kinase-inactivating mutant of RIP3 (K50A) (He et al., 2009; Wang et al., 2012) also lost the ability to interact with PELI1 (Figure 5K) and was protected from PELI1-induced degradation (Figure 5L) and polyubiquitylation (Figure S4G). In contrast, ubiquitylation of RIP3 by CHIP was unaffected by the K50A mutation (Figure S4H); CHIP-mediated degradation of this mutant was only slightly reduced, and dabrafenib treatment did not affect the degradation of WT RIP3 mediated by CHIP (Figures 5M and S4I). These data indicate that PELI1 requires RIP3 kinase activity in order to target RIP3 for degradation, while CHIP has no such requirement.

## pT 182 Is Important for Regulating RIP3 Kinase Activity

We postulated that phospho-T182 could function as a priming site for the auto-phosphorylation of Ser-227. To test this, we purified baculovirus-expressed recombinant human RIP3 kinase domain (amino acids [aa] 2–328) and mutants in insect cells. The recombinant WT kinase domain was active as measured by the auto-phosphorylation of Ser-227 (Figure 6A); this activity increased somewhat in the presence of *in vitro* kinase assay components (Figure 6B). However, as in mammalian cells, the T182A mutant protein lost this activity, similar to the kinase-deficient mutation, K50A (Figures 6A and 6B). We next detected auto-phosphorylation events in an *in vitro* kinase assay using [$\gamma$-$^{32}$P] ATP (Figure 6C). As expected, RIP3 (K50A) did not possess any kinase activity; RIP3 (T182A) lost most of its activity, while RIP3 (S227) had only partially reduced kinase activity (Figure 6C). Similar results were obtained in 293T cells when FLAG-tagged RIP3 constructs were immunoprecipitated and subjected to an *in vitro* kinase assay visualized by autoradiography, with the only $^{32}$P-labeled band found in the

(E) FLAG-RIP3 and/or HA-Ub were transfected into 293T cells in the absence or presence of GFP-tagged WT or R104A PELI1 for 20 hr. Transfected cells were exposed to 10 μM MG132 for the final 3 hr of incubation.
(F) 293T cells were transfected with FLAG-RIP3 WT or mutants (T182A, T200A, T224A, T300A, T325A, T369A and T387A) in the absence or presence of Myc-PELI1 for 24h. Cell lysates were analyzed by western blotting. GFP was used as a transfection control.
(G) HeLa cells were transfected with FLAG-tagged RIP3 WT or mutants (T182A, T200A and T224A) with or without Myc-PELI1. After 36 hr, cell lysates were analyzed by western blotting. A GFP expressing plasmid was used as a transfection control.
(H) FLAG-tagged WT, T182A, T200A, or T224A RIP3 was transfected into 293T cells in the absence or presence of Myc-PELI1. After 20 hr, which included a final 3 hr of 10 μM MG132 incubation, cell lysates were immunoprecipitated with an anti-Myc antibody.
(I) FLAG-tagged WT, T182A, T200A or T224A RIP3 was transfected into 293T cells with HA-Ub in the absence or presence of the GFP-PELI1 for 20 hr. Transfected cells were exposed to 10 μM MG132 for the final 3 hr of incubation. Cell lysates were immunoprecipitated with an anti-FLAG antibody.

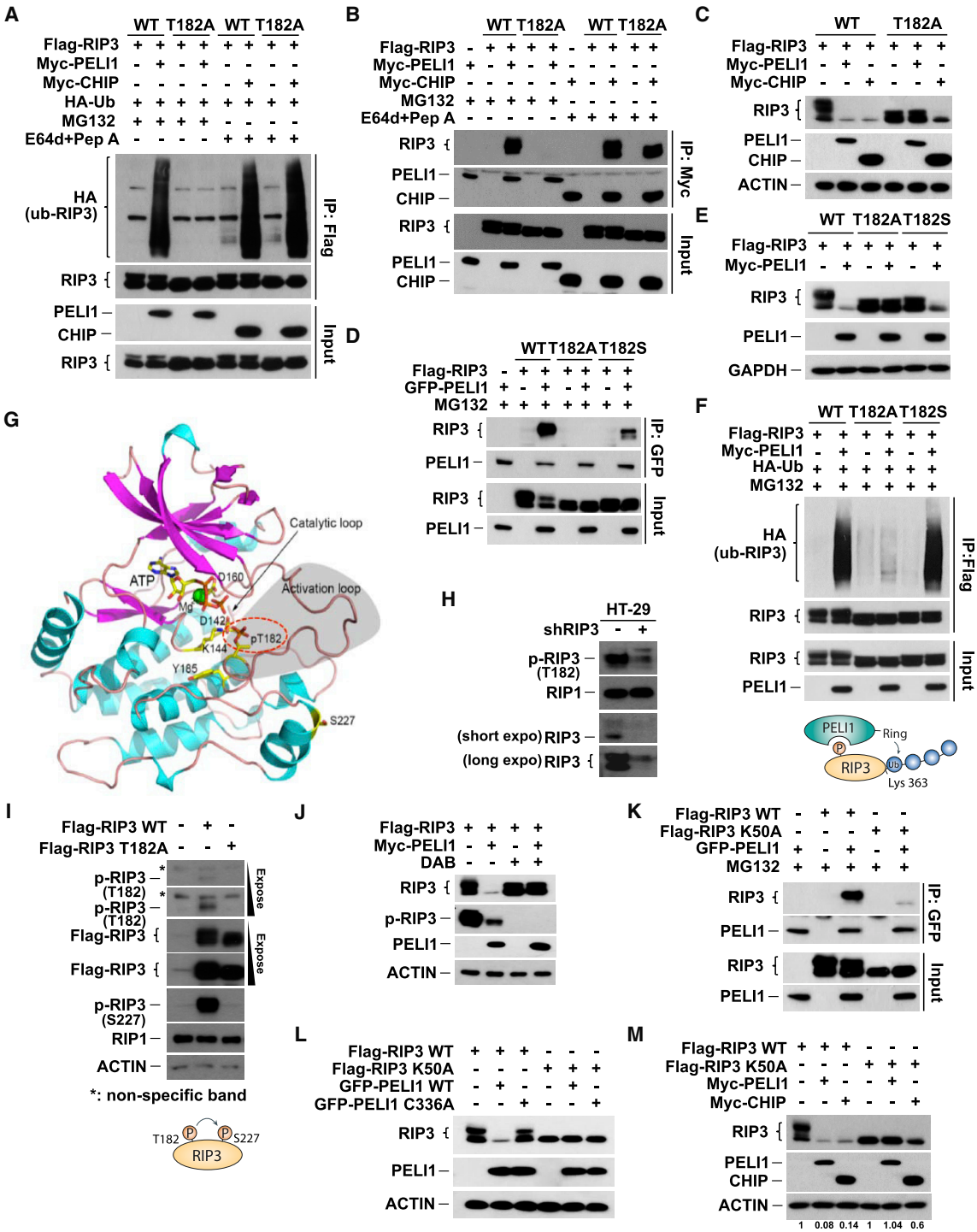


**Figure 5. T182 of RIP3 Is Indispensable for the RIP3-PELI1 Interaction and for RIP3 Ubiquitylation and Degradation**

(A) 293T cells were transfected with FLAG-RIP3, HA-Ub, and Myc-PELI1 or Myc-CHIP and then treated with or without MG132 or E64d + pepstatin. Lysates were immunoprecipitated with an anti-FLAG antibody (18 hr).

(B) FLAG-RIP3 was transfected into 293T cells with Myc-PELI1 or Myc-CHIP in the presence of MG132 or E64d + pepstatin. Lysates were immunoprecipitated with an anti-Myc antibody (18 hr).

(C) FLAG-tagged WT or T182A RIP3 was transfected into 293T cells with Myc-PELI1 or Myc-CHIP. After 24 hr, lysates were analyzed by western blotting.

(D) FLAG-tagged WT, T182A, or T182S RIP3 was transfected into 293T cells in the absence or presence of GFP-PELI1. After 20 hr, and a final 3 hr of 10 μM MG132 incubation, lysates were immunoprecipitated with an anti-GFP antibody.

*(legend continued on next page)*

WT RIP3 and the S227A mutant lanes (Figure 6D, left panel). Taken together, these results suggest that T182 is an important amino acid for RIP3 kinase activity.

### Disruption in T182 Inhibits S227 Auto-phosphorylation and TNF-Induced Necroptosis

We next verified the consequences of the T182A mutation on necroptosis. FLAG-tagged RIP3 (T182A) maintained its ability to interact with RIP1 in co-immunoprecipitation assays but was unable to interact with MLKL; the T182S mutant maintained interaction with both RIP1 and MLKL (Figure 6E). Consistent with our previous results, S227 phosphorylation was abrogated by T182A mutation in both 293T cell and HeLa cells upon RIP3 overexpression (Figures 6F and 6G). Unlike WT RIP3, ectopic expression of the T182A mutant was unable to rescue MLKL phosphorylation induced by the necroptotic stimulus TSZ (TNF-α + SMAC mimetic + zVAD) in HeLa cells, which lack endogenous RIP3 expression (Figure 6H). As expected, T182A was unable to restore TNF-induced necroptosis in HeLa cells and had no effect on TNF-induced apoptosis (TS alone), though the WT RIP3 fully restored necroptosis (Figure 6I). Taken together, our data suggest that T182A RIP3 is unable to mediate TNF-induced necroptosis, consistent with its lack of kinase activity.

### PELI1-Mediated RIP3 Degradation Abolishes Necroptotic Cell Death

Based on our results, we would expect downregulation of RIP3 protein by PELI1 would inhibit RIP3-MLKL-dependent necroptotic cell death and, in turn, maintain cell survival. Spontaneous cell death induced by RIP3 overexpression was suppressed by PELI1, but not its C336A-ligase-defective mutant (Figures S5A and S5B). Knockdown of PELI1 led to more potent RIP3 and MLKL phosphorylation in response to necroptotic stimuli (TSZ or TNF-α+cycloheximide+zVAD [TCZ] treatment) and also made HT-29 cells more sensitive to cell death (Figures 7A, S5C, and S5D), while the necroptosis inhibitor necrostatin-1 (a RIP1 inhibitor) completely abolished the increased MLKL phosphorylation and additional cell death potentiated by PELI1 knockdown (Figure S5D). Moreover, PELI1 knockout MEFs had a more potent MLKL phosphorylation and additional necroptotic cell death in response to TNF compared to WT cells (Figures 7B, S5E, and S5F). Importantly, endogenous PELI1 interacted with RIP3 and RIP1 in the necrosome complex upon TSZ treatment in both HT-29 and MEFs (Figures 7C, S6A, and S6B).

As expected, the endogenous amount of basal RIP3 expression was increased in HT-29, Jurkat, and PELI1 MEFs upon PELI1 knockdown/knockout (Figures S6C–S6E). PELI1 expression remained unaltered during TNF-induced necroptosis (Figure S10A). In the absence of exogenous stimuli, we could detect a basal amount of RIP3 and MLKL phosphorylation in some cell types with high RIP3 expression (e.g., HT-29), although the amounts of these phospho-species were much lower than during stimuli-induced activation (Figure S7B). This basal amount was eliminated by the RIP3 inhibitor dabrafenib, but not the RIP1 inhibitor necrostatin-1 (Figure S7B). The fact that small amounts of dabrafenib-sensitive MLKL phosphorylation could be achieved by overexpression of RIP3 in RIP1/RIP3-deficient MEFs (Figure S7C) suggests that this level of activation could be achieved independent of receptor stimulation when RIP3 levels are high and suggests that inopportune necroptosis could happen when RIP3 expression is misregulated. The small amount of MLKL and RIP3 phosphorylation were both increased when endogenous PELI1 expression was suppressed by shRNA (Figure 7D) or small interfering RNA (siRNA) (Figure 7E). Conversely, ectopically expressed PELI1 diminished RIP3 expression as well as RIP3 and MLKL phosphorylation (Figures 7F and S7D). Lung tissues from PELI1 transgenic (Tg) mice show a decrease in basal MLKL phosphorylation indicating that upregulated PELI1 may function to preferentially remove activated RIP3 and reduce MLKL phosphorylation *in vivo* (Figure S7E). This suggests that PELI1 may play a role in maintaining cellular homeostasis by preventing improper RIP3 activation and maintaining a higher cell death threshold.

### Low Expression of PELI1 Potentiates RIP3 Expression in TEN Keratinocytes

We previously reported that elevated RIP3 expression potentiates MLKL-mediated necroptosis in TEN (Kim et al., 2015), a life-threatening dermatological disorder usually caused by drug reaction and characterized by extensive keratinocyte death with separation at the dermoepidermal junction (Downey et al.,

(E) 293T cells were transfected with FLAG-tagged RIP3 WT or mutants (T182A and T182S) with or without Myc-PELI1 and lysates analyzed by western blotting (20 hr).
(F) FLAG-tagged WT, T182A, or T182S RIP3 was transfected with HA-Ub into 293T cells in the presence or absence of Myc-tagged PELI1 (20 hr) with 10 μM MG132 for the final 3 hr. Lysates were immunoprecipitated with an anti-FLAG antibody.
(G) Ribbon diagram illustrating the important residues in a human RIP3 model. α helices and β strands are colored cyan and magenta, respectively. Side chains of mutated residues and bound ATP are illustrated using a stick model with carbon, nitrogen, oxygen, and phosphate atoms colored yellow, blue, red, and orange, respectively. Magnesium is shown as a green ball. Catalytic and activation loops and phosphorylated Thr182 are indicated.
(H) Lysates of HT-29 cells stably expressing RIP3 shRNA or non-silencing control were analyzed by western blotting.
(I) Lysates of 293T cells transfected with FLAG-RIP3 WT or T182A mutant were analyzed by western blotting (24 hr).
(J) 293T cells were transfected with FLAG-RIP3 and/or Myc-PELI1 in the absence or presence of 10 μM dabrafenib for 24 hr; cell lysates were analyzed by western blotting.
(K) 293T cells were transfected with FLAG-RIP3 WT and K50A mutant in the absence or presence of GFP-PELI1 for 20 hr, including a final 3 hr 10 μM MG132 incubation. Cell lysates were immunoprecipitated with an anti-GFP antibody.
(L) 293T cells were transfected with FLAG-RIP3 WT and K50A mutant in the absence or presence of GFP-PELI1 WT or C336A mutant. After 24 hr, cell lysates were analyzed by western blotting.
(M) Expression plasmids for FLAG-RIP3 WT or K50A mutant were transfected into 293T cells in the absence or presence of Myc-PELI1 or Myc-CHIP. After 24 hr, cell lysates were analyzed by western blotting.

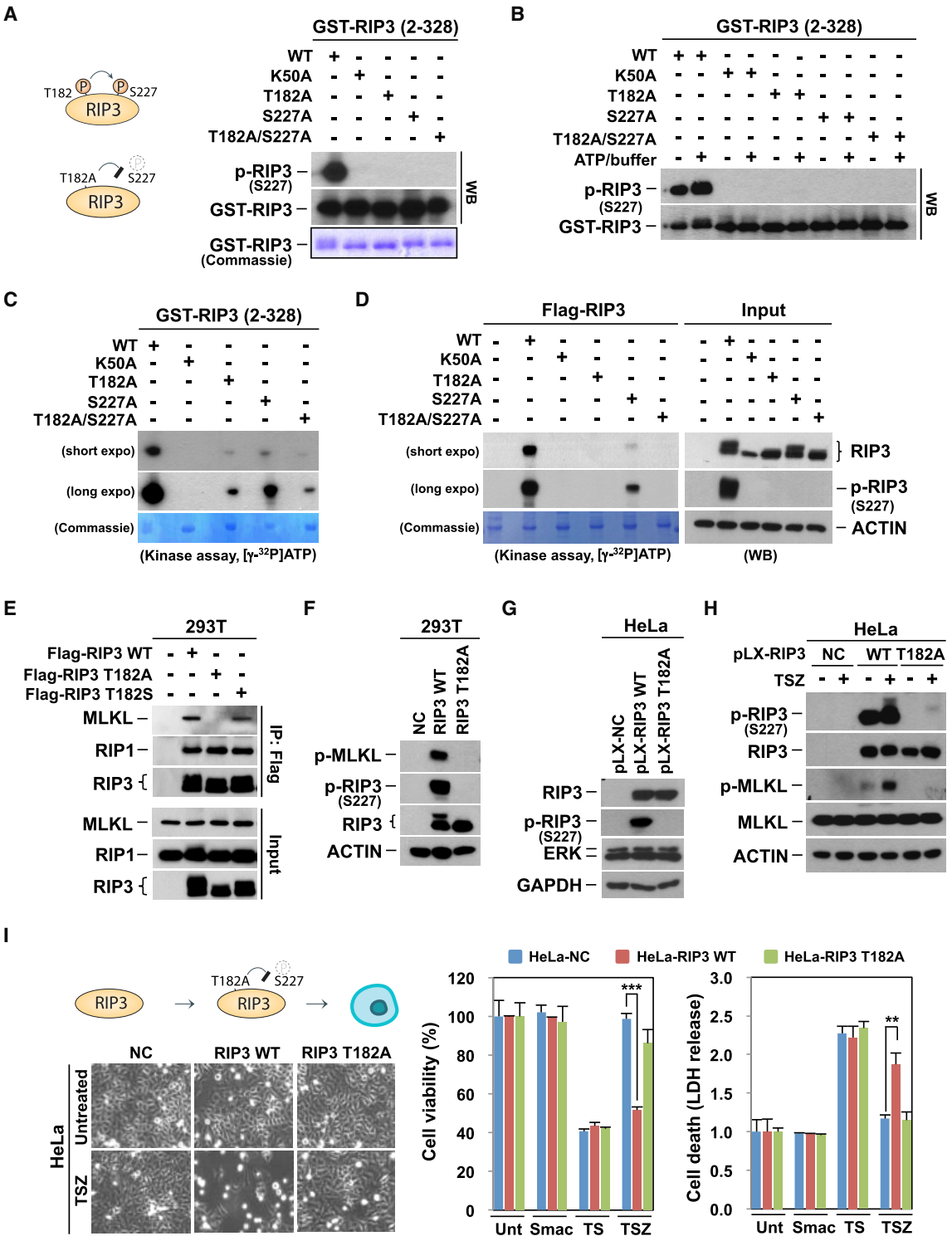


**Figure 6. T182 Is the Important Amino Acid for Regulating RIP3 Kinase Activity and TNF-Induced Necroptosis**

(A and B) Purified baculovirus-expressed recombinant wild-type or mutant human RIP3 kinase domain (amino acids [aa] 2–328) proteins were analyzed for kinase activity by western blotting (A) or *in vitro* kinase assays (B).

(C) Purified baculovirus-expressed recombinant wild-type or mutant human RIP3 kinase domain (amino acids [aa] 2–328) proteins were analyzed for *in vitro* kinase activity using the [$\gamma^{32}$P] ATP. Kinase activity was determined by autoradiography.

*(legend continued on next page)*

2012; Pereira et al., 2007; Schwartz et al., 2013). The Human Protein Atlas indicated that PELI1 expression is typically high in skin tissue, so we hypothesized that PELI1 negatively regulates necroptosis through ubiquitylating RIP3. PELI1 siRNA did indeed increase the endogenous amounts of RIP3 protein in keratinocytes (Figures 7G and S7F), and RIP3 expression was diminished by PELI1 WT expression, but not by PELI1 C336A, in these cells (Figure 7H). RIP3 protein and phosphorylated MLKL levels are markedly increased in skin from TEN patients compared with normal skin; TNF- and SNP-induced necroptosis in keratinocytes are attenuated by the RIP3 inhibitor dabrafenib (Kim et al., 2015). Immunohistochemical staining verified that PELI1 was high in normal skin but decreased in TEN patients (Figure 7I, left panel). Quantification using image analysis (pigmented area per measured epidermal area) suggested upregulated RIP3 expression was correlated with decreased PELI1 expression in the TEN patients; RIP3 was increased in the TEN skin compared with normal skin, where PELI1 was more highly expressed, suggesting that RIP3 expression level was negatively regulated by PELI1 in patients (Figure 7I, right panel).

## DISCUSSION

Pellino proteins, such as PELI1, have been known to catalyze the addition of K48- or K63-linked ubiquitin chains to proteins of the innate and adaptive immune systems (Chang et al., 2009; Conze et al., 2008; Moynagh, 2009; Schauvliege et al., 2006). For instance, stimulation of TLR3 or TLR4 triggers interaction of RIP1 with TRIF through its RHIM domain, and this event is followed by recruitment of PELI1, which mediates K63-linked RIP1 polyubiquitylation; subsequent recruitment of TAK-1 and IKK complexes to this polyubiquitin chain leads to the expression of pro-inflammatory genes (Chang et al., 2009; Cusson-Hermance et al., 2005; Goh et al., 2012). Here, we show that RIP3 also interacts with PELI1; however, PELI1 modulates the protein stability of RIP3 rather than mediating signaling events, because it ubiquitylates RIP3 by K48-linked ubiquitin chains rather than K63-linked chains. RIP3 ubiquitylation and degradation by this mechanism (Figure 7J) may prevent unnecessary cell death by RIP3 and maintain cellular homeostasis.

A previous report indicates that the ubiquitinylase CHIP controls RIP3 expression (Seo et al., 2016) by ubiquitylation and lysosome-mediated degradation. While we were unable to observe upregulation of endogenous RIP3 expression in response to lysosomal inhibition, we were able to observe CHIP-dependent ubiquitylation and degradation in overexpression assays. However, there were significant differences in recognition of RIP3 by the two ubiquitin ligases. PELI1 requires RIP3 T182 for recognition; CHIP does not. PELI1 preferentially recognizes and mediates the degradation of phosphorylated RIP3 that is dependent on phospho-T182; CHIP seems to recognize and cause degradation of both forms of RIP3 equally. PELI1 recognition of RIP3 requires that RIP3 be kinase proficient; CHIP has no such requirement. Thus, CHIP and PELI1 control the stability of RIP3 in different states. We hypothesize that coordination of the activities allow for fine control of RIP3 expression in inactivated and activated RIP3, respectively.

In the midst of the conclusion of our studies, an article was published that suggested the reverse conclusion that PELI1 deficiency actually blocked necroptosis; PELI1 was suggested to be required for necroptosis because its ubiquitylation of RIP1 on K115 was necessary for RIP1 binding to and activating RIP3 and thus activation of MLKL (Wang et al., 2017). The reason for this discrepancy with our study is unclear. Loss or reduction of RIP3 expression can occur in passaged MEF cell lines, such as has been demonstrated in some passages of RIP1 knockout (KO) MEF cells (Morgan and Kim, 2015; Zhang et al., 2011), which often lead to confusing results with regards to effects of gene KO on necroptosis. We have shown herein that PELI1 KO cells do die in response to TNF-dependent necroptosis (Figures 7B, S5E, and S5F), that they actually respond to stimulation with increased (rather than decreased) phospho-MLKL (Figure 7B), and that the necrosome complex, including the RIP1-RIP3 interaction, is efficiently formed in PELI1 KO cells (Figure S6B).

In the absence of exogenous stimuli, high RIP3 expression has been reported to lead to spontaneous auto-phosphorylation and inopportune necroptosis (Chen et al., 2015); cells may need compensation mechanisms to prevent this occurrence, and PELI1-mediated degradation of kinase active RIP3 may represent one mechanism by which to achieve this. Our data show that low expression of PELI1 results in high expression of RIP3 in keratinocytes; this may contribute to necrotic cell death in TEN patients via MLKL activation. Our findings suggest that maintaining PELI1 expression in keratinocytes should help to prevent keratinocyte death and may be a therapeutic target for TEN (Kim et al., 2015).

PELI1 Tg mice develop a wide range of tumors (Park et al., 2014). We have previously reported that RIP3 expression is lost in many cancer cell lines and primary breast cancers and is negatively selected against during initial tumor development or growth (Koo et al., 2015). In patients, PELI1 overexpression is closely associated with poor prognosis in diffuse large B cell lymphoma (DLBCLs) (Park et al., 2014), suggesting that PELI1 could provide a selective advantage during

(D) 293T cells were transfected with FLAG-tagged RIP3, RIP3 (K50A), RIP3 (T182A), RIP3 (S227A), or RIP3 (T182A/S227A), and immunoprecipitated RIP3 was subjected to an *in vitro* kinase assay and visualized by autoradiography.

(E) 293T cells were transfected with FLAG-tagged RIP3, RIP3 (T182A), or RIP3 (T182S). Cell lysates were immunoprecipitated with an anti-FLAG antibody.

(F) 293T cells were transfected with FLAG-tagged RIP3 or RIP3 (T182A). Cell lysates were analyzed by western blotting.

(G) HeLa cells ectopically expressing RIP3 wild-type or T182 mutant were established, and cell lysates were analyzed by western blotting.

(H) Cells from (G) were treated with TSZ for 6 hr, and cell lysates were analyzed by western blotting.

(I) Cells from (G) were treated with TS or TSZ for 24 hr, and cell viability was analyzed using a (3-(4,5-Dimethylthiazol-2-yl)-2,5-Diphenyltetrazolium Bromide) (MTT) assay or a CellTiter-Glo Luminescent Cell Viability Assay Kit (right). Data are presented as mean ± SEM. *$p < 0.05$, **$p < 0.01$, ***$p < 0.001$. Cell viability was also analyzed by phase-contrast microscopy.

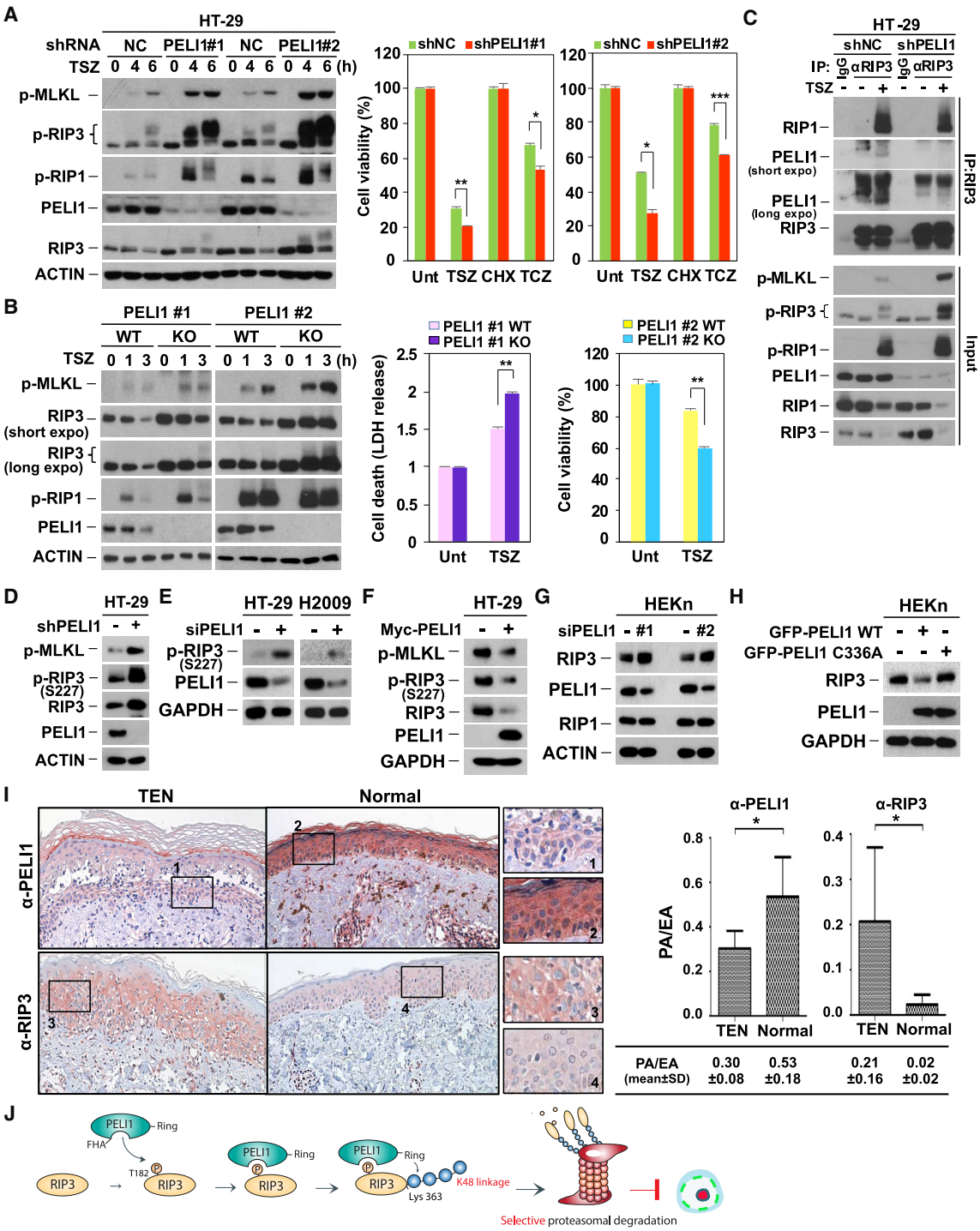


**Figure 7. PELI1 Regulates Unnecessary Necroptosis by Reducing RIP3 Expression**

(A) HT-29 cells stably expressing PELI1 shRNA (#1 and #2) or non-silencing control were treated with TSZ for indicated times. The cells were harvested and total lysates were analyzed by western blotting (left). Cells were treated with TSZ or TCZ for 24 hr and cell viability was analyzed by MTT assay (right). Data are presented as mean ± SEM. *$p < 0.05$, **$p < 0.01$, ***$p < 0.01$.

(B) PELI1 wild-type and knockout MEFs (#1 and #2) were treated with TSZ for indicated times. The cells were harvested and total lysates were analyzed by western blotting (left). Cells were treated with TSZ for 24 hr and cell viability was analyzed by MTT assay or CellTiter-Glo Luminescent Cell Viability Assay (right). Data are presented as mean ± SEM. *$p < 0.05$, **$p < 0.01$, ***$p < 0.01$.

(C) Cells from (A) were treated with TSZ for 4 hr, and cell lysates were immunoprecipitated with anti-RIP3 antibody.

*(legend continued on next page)*

tumor-growth-dependent through downregulation of RIP3. A better understanding of the regulation of post-translational modification of RIP3 may thus not only aid in the development of drugs for various necroptosis-related diseases but also provide further insights into possible tumor-suppressive effects of RIP3 in cancer.

## STAR★METHODS

Detailed methods are provided in the online version of this paper and include the following:

- KEY RESOURCES TABLE
- CONTACT FOR REAGENT AND RESOURCE SHARING
- METHOD DETAILS
  - Cell lines and culture conditions
  - Antibodies and chemical reagents
  - Plasmid construction, mutagenesis, and transfection
  - siRNA, shRNA, and reverse transcription-PCR (RT-PCR)
  - Cytotoxicity Assays
  - Immunoprecipitation and immunoblot analysis
  - *In vitro* ubiquitylation assay
  - Protein Microarray
  - Mass Spectrometric Analysis
  - RIP3 structure modeling
  - Purification of recombinant proteins
  - *In vitro* kinase assays
  - Immunohistochemistry and Image analysis
- DATA AND SOFTWARE AVAILABILITY
- QUANTIFICATION AND STATISTICAL ANALYSIS

## SUPPLEMENTAL INFORMATION

Supplemental Information includes seven figures and one table and can be found with this article online at https://doi.org/10.1016/j.molcel.2018.05.016.

## ACKNOWLEDGMENTS

We thank Shao-Cong Sun for PELI1KO MEFs. This work was supported by a National Research Foundation of Korea (NRF) grant funded by the Korea government (2011-0030043, 2017R1A2B3002343) and a grant from the Korea Health Technology R&D Project through the Korea Health Industry Development Institute (KHIDI), funded by the Ministry of Health & Welfare, Republic of Korea (HI15C0554).

## AUTHOR CONTRIBUTIONS

S.-W.C. and H.-H.P. performed the majority of cellular and biochemical experiments. S.K. and J.M.C. performed protein array and *in vitro* Ub assays. H.-J.N. performed a number of biochemical studies. S.K.K. analyzed TNE patient samples. H.K.S. analyzed RIP3 crystal structure. C.-W.L. provided reagents and mice. M.J.M. analyzed data and contributed to manuscript writing. H.C.K. and Y.-S.K. conceived and coordinated all studies and wrote the paper with input from coauthors.

## DECLARATION OF INTERESTS

The authors declare no competing interests.

Received: November 27, 2017
Revised: March 13, 2018
Accepted: May 15, 2018
Published: June 7, 2018

## REFERENCES

Aaes, T.L., Kaczmarek, A., Delvaeye, T., De Craene, B., De Koker, S., Heyndrickx, L., Delrue, I., Taminau, J., Wiernicki, B., De Groote, P., et al. (2016). Vaccination with necroptotic cancer cells induces efficient anti-tumor immunity. Cell Rep. *15*, 274–287.

Bonnet, M.C., Preukschat, D., Welz, P.S., van Loo, G., Ermolaeva, M.A., Bloch, W., Haase, I., and Pasparakis, M. (2011). The adaptor protein FADD protects epidermal keratinocytes from necroptosis in vivo and prevents skin inflammation. Immunity *35*, 572–582.

Borden, K.L., and Freemont, P.S. (1996). The RING finger domain: a recent example of a sequence-structure family. Curr. Opin. Struct. Biol. *6*, 395–401.

Cai, Z., Jitkaew, S., Zhao, J., Chiang, H.C., Choksi, S., Liu, J., Ward, Y., Wu, L.G., and Liu, Z.G. (2014). Plasma membrane translocation of trimerized MLKL protein is required for TNF-induced necroptosis. Nat. Cell Biol. *16*, 55–65.

Chang, M., Jin, W., and Sun, S.C. (2009). Peli1 facilitates TRIF-dependent Toll-like receptor signaling and proinflammatory cytokine production. Nat. Immunol. *10*, 1089–1095.

Chang, M., Jin, W., Chang, J.H., Xiao, Y., Brittain, G.C., Yu, J., Zhou, X., Wang, Y.H., Cheng, X., Li, P., et al. (2011). The ubiquitin ligase Peli1 negatively regulates T cell activation and prevents autoimmunity. Nat. Immunol. *12*, 1002–1009.

Chen, X., Li, W., Ren, J., Huang, D., He, W.T., Song, Y., Yang, C., Li, W., Zheng, X., Chen, P., and Han, J. (2014). Translocation of mixed lineage kinase domain-like protein to plasma membrane leads to necrotic cell death. Cell Res. *24*, 105–121.

Chen, W., Wu, J., Li, L., Zhang, Z., Ren, J., Liang, Y., Chen, F., Yang, C., Zhou, Z., Su, S.S., et al. (2015). Ppm1b negatively regulates necroptosis through dephosphorylating Rip3. Nat. Cell Biol. *17*, 434–444.

Cho, Y.S., Challa, S., Moquin, D., Genga, R., Ray, T.D., Guildford, M., and Chan, F.K. (2009). Phosphorylation-driven assembly of the RIP1-RIP3 complex regulates programmed necrosis and virus-induced inflammation. Cell *137*, 1112–1123.

Conze, D.B., Wu, C.J., Thomas, J.A., Landstrom, A., and Ashwell, J.D. (2008). Lys63-linked polyubiquitination of IRAK-1 is required for interleukin-1 receptor- and toll-like receptor-mediated NF-kappaB activation. Mol. Cell. Biol. *28*, 3538–3547.

Cusson-Hermance, N., Khurana, S., Lee, T.H., Fitzgerald, K.A., and Kelliher, M.A. (2005). Rip1 mediates the Trif-dependent toll-like receptor 3- and 4-induced NF-kappaB activation but does not contribute to interferon regulatory factor 3 activation. J. Biol. Chem. *280*, 36560–36566.

(D) HT-29 cells were infected with lentiviral particles containing shRNA against either PELI1 or control for 48 hr. Cell lysates were analyzed by western blotting.
(E) HT-29 (left panel) or H2009 (right panel) cells were transfected with control or PELI1 siRNAs for 48 hr, and total lysates were analyzed by western blotting.
(F) HT-29 cells were transfected with Myc-tagged empty vector or PELI1. After 48 hr of transfection, cell lysates were analyzed by western blotting.
(G) Human epidermal keratinocytes (HEKn) were transfected with control or PELI1 siRNAs for 48 hr, and total lysates were analyzed by western blotting.
(H) Expression vehicles for GFP-tagged PELI1-WT or -C336A mutant were transfected into HEKn cells for 36 hr, and total cell lysate analyzed by western blotting.
(I) Immunohistochemical staining indicates RIP3 and PELI1 expression are inversely correlated in TEN skin compared with normal skin (left). Quantitative image analysis of RIP3 and PELI1 staining (right). PA/EA, pigmented area per measured epidermal area.
(J) Schematic diagram of a novel, proteasome-dependent mode of RIP3 degradation mediated by an E3 ubiquitin ligase (PELI1).

Deshaies, R.J., and Joazeiro, C.A. (2009). RING domain E3 ubiquitin ligases. Annu. Rev. Biochem. *78*, 399–434.

Downey, A., Jackson, C., Harun, N., and Cooper, A. (2012). Toxic epidermal necrolysis: review of pathogenesis and management. J. Am. Acad. Dermatol. *66*, 995–1003.

Durocher, D., Henckel, J., Fersht, A.R., and Jackson, S.P. (1999). The FHA domain is a modular phosphopeptide recognition motif. Mol. Cell *4*, 387–394.

Durocher, D., Taylor, I.A., Sarbassova, D., Haire, L.F., Westcott, S.L., Jackson, S.P., Smerdon, S.J., and Yaffe, M.B. (2000). The molecular basis of FHA domain:phosphopeptide binding specificity and implications for phospho-dependent signaling mechanisms. Mol. Cell *6*, 1169–1182.

Gardam, S., Sierro, F., Basten, A., Mackay, F., and Brink, R. (2008). TRAF2 and TRAF3 signal adapters act cooperatively to control the maturation and survival signals delivered to B cells by the BAFF receptor. Immunity *28*, 391–401.

Goh, E.T., Arthur, J.S., Cheung, P.C., Akira, S., Toth, R., and Cohen, P. (2012). Identification of the protein kinases that activate the E3 ubiquitin ligase Pellino 1 in the innate immune system. Biochem. J. *441*, 339–346.

Grech, A.P., Amesbury, M., Chan, T., Gardam, S., Basten, A., and Brink, R. (2004). TRAF2 differentially regulates the canonical and noncanonical pathways of NF-kappaB activation in mature B cells. Immunity *21*, 629–642.

Guex, N., Peitsch, M.C., and Schwede, T. (2009). Automated comparative protein structure modeling with SWISS-MODEL and Swiss-PdbViewer: a historical perspective. Electrophoresis *30* (*Suppl 1*), S162–S173.

Günther, C., Martini, E., Wittkopf, N., Amann, K., Weigmann, B., Neumann, H., Waldner, M.J., Hedrick, S.M., Tenzer, S., Neurath, M.F., and Becker, C. (2011). Caspase-8 regulates TNF-$\alpha$-induced epithelial necroptosis and terminal ileitis. Nature *477*, 335–339.

He, S., Wang, L., Miao, L., Wang, T., Du, F., Zhao, L., and Wang, X. (2009). Receptor interacting protein kinase-3 determines cellular necrotic response to TNF-alpha. Cell *137*, 1100–1111.

Huoh, Y.S., and Ferguson, K.M. (2014). The pellino e3 ubiquitin ligases recognize specific phosphothreonine motifs and have distinct substrate specificities. Biochemistry *53*, 4946–4955.

Kaiser, W.J., Upton, J.W., Long, A.B., Livingston-Rosanoff, D., Daley-Bauer, L.P., Hakem, R., Caspary, T., and Mocarski, E.S. (2011). RIP3 mediates the embryonic lethality of caspase-8-deficient mice. Nature *471*, 368–372.

Kim, Y.S., Morgan, M.J., Choksi, S., and Liu, Z.G. (2007). TNF-induced activation of the Nox1 NADPH oxidase and its role in the induction of necrotic cell death. Mol. Cell *26*, 675–687.

Kim, S.K., Kim, W.J., Yoon, J.H., Ji, J.H., Morgan, M.J., Cho, H., Kim, Y.C., and Kim, Y.S. (2015). Upregulated RIP3 expression potentiates MLKL phosphorylation-mediated programmed necrosis in toxic epidermal necrolysis. J. Invest. Dermatol. *135*, 2021–2030.

Kim, D., Lee, H., Koh, J., Ko, J.S., Yoon, B.R., Jeon, Y.K., Cho, Y.M., Kim, T.H., Suh, Y.-S., Lee, H.-J., et al. (2017). Cytosolic Pellino-1-mediated K63-linked ubiquitination of IRF5 in M1 macrophages regulates glucose intolerance in obesity. Cell Rep. *20*, 832–845.

Koo, G.B., Morgan, M.J., Lee, D.G., Kim, W.J., Yoon, J.H., Koo, J.S., Kim, S.I., Kim, S.J., Son, M.K., Hong, S.S., et al. (2015). Methylation-dependent loss of RIP3 expression in cancer represses programmed necrosis in response to chemotherapeutics. Cell Res. *25*, 707–725.

Li, J., Lee, G.I., Van Doren, S.R., and Walker, J.C. (2000). The FHA domain mediates phosphoprotein interactions. J. Cell Sci. *113*, 4143–4149.

Li, J., McQuade, T., Siemer, A.B., Napetschnig, J., Moriwaki, K., Hsiao, Y.S., Damko, E., Moquin, D., Walz, T., McDermott, A., et al. (2012). The RIP1/RIP3 necrosome forms a functional amyloid signaling complex required for programmed necrosis. Cell *150*, 339–350.

Li, J.X., Feng, J.M., Wang, Y., Li, X.H., Chen, X.X., Su, Y., Shen, Y.Y., Chen, Y., Xiong, B., Yang, C.H., et al. (2014). The B-Raf(V600E) inhibitor dabrafenib selectively inhibits RIP3 and alleviates acetaminophen-induced liver injury. Cell Death Dis. *5*, e1278.

Lin, C.C., Huoh, Y.S., Schmitz, K.R., Jensen, L.E., and Ferguson, K.M. (2008). Pellino proteins contain a cryptic FHA domain that mediates interaction with phosphorylated IRAK1. Structure *16*, 1806–1816.

Mocarski, E.S., Upton, J.W., and Kaiser, W.J. (2011). Viral infection and the evolution of caspase 8-regulated apoptotic and necrotic death pathways. Nat. Rev. Immunol. *12*, 79–88.

Mocarski, E.S., Kaiser, W.J., Livingston-Rosanoff, D., Upton, J.W., and Daley-Bauer, L.P. (2014). True grit: programmed necrosis in antiviral host defense, inflammation, and immunogenicity. J. Immunol. *192*, 2019–2026.

Morgan, M.J., and Kim, Y.S. (2015). The serine threonine kinase RIP3: lost and found. BMB Rep. *48*, 303–312.

Morgan, M.J., and Liu, Z.G. (2013). Programmed cell death with a necrotic-like phenotype. Biomol. Concepts *4*, 259–275.

Moynagh, P.N. (2009). The Pellino family: IRAK E3 ligases with emerging roles in innate immune signalling. Trends Immunol. *30*, 33–42.

Onizawa, M., Oshima, S., Schulze-Topphoff, U., Oses-Prieto, J.A., Lu, T., Tavares, R., Prodhomme, T., Duong, B., Whang, M.I., Advincula, R., et al. (2015). The ubiquitin-modifying enzyme A20 restricts ubiquitination of the kinase RIPK3 and protects cells from necroptosis. Nat. Immunol. *16*, 618–627.

Ordureau, A., Smith, H., Windheim, M., Peggie, M., Carrick, E., Morrice, N., and Cohen, P. (2008). The IRAK-catalysed activation of the E3 ligase function of Pellino isoforms induces the Lys63-linked polyubiquitination of IRAK1. Biochem. J. *409*, 43–52.

Park, H.Y., Go, H., Song, H.R., Kim, S., Ha, G.H., Jeon, Y.K., Kim, J.E., Lee, H., Cho, H., Kang, H.C., et al. (2014). Pellino 1 promotes lymphomagenesis by deregulating BCL6 polyubiquitination. J. Clin. Invest. *124*, 4976–4988.

Pereira, F.A., Mudgil, A.V., and Rosmarin, D.M. (2007). Toxic epidermal necrolysis. J. Am. Acad. Dermatol. *56*, 181–200.

Schauvliege, R., Janssens, S., and Beyaert, R. (2006). Pellino proteins are more than scaffold proteins in TLR/IL-1R signalling: a role as novel RING E3-ubiquitin-ligases. FEBS Lett. *580*, 4697–4702.

Schwartz, R.A., McDonough, P.H., and Lee, B.W. (2013). Toxic epidermal necrolysis: Part II. Prognosis, sequelae, diagnosis, differential diagnosis, prevention, and treatment. J. Am. Acad. Dermatol. *69*, 187.e1–16; quiz 203–204.

Seo, J., Lee, E.W., Sung, H., Seong, D., Dondelinger, Y., Shin, J., Jeong, M., Lee, H.K., Kim, J.H., Han, S.Y., et al. (2016). CHIP controls necroptosis through ubiquitylation- and lysosome-dependent degradation of RIPK3. Nat. Cell Biol. *18*, 291–302.

Vanden Berghe, T., Linkermann, A., Jouan-Lanhouet, S., Walczak, H., and Vandenabeele, P. (2014). Regulated necrosis: the expanding network of non-apoptotic cell death pathways. Nat. Rev. Mol. Cell Biol. *15*, 135–147.

Vandenabeele, P., Galluzzi, L., Vanden Berghe, T., and Kroemer, G. (2010). Molecular mechanisms of necroptosis: an ordered cellular explosion. Nat. Rev. Mol. Cell Biol. *11*, 700–714.

Vanlangenakker, N., Vanden Berghe, T., and Vandenabeele, P. (2012). Many stimuli pull the necrotic trigger, an overview. Cell Death Differ. *19*, 75–86.

Wang, Z., Jiang, H., Chen, S., Du, F., and Wang, X. (2012). The mitochondrial phosphatase PGAM5 functions at the convergence point of multiple necrotic death pathways. Cell *148*, 228–243.

Wang, H., Sun, L., Su, L., Rizo, J., Liu, L., Wang, L.F., Wang, F.S., and Wang, X. (2014). Mixed lineage kinase domain-like protein MLKL causes necrotic membrane disruption upon phosphorylation by RIP3. Mol. Cell *54*, 133–146.

Wang, H., Meng, H., Li, X., Zhu, K., Dong, K., Mookhtiar, A.K., Wei, H., Li, Y., Sun, S.-C., and Yuan, J. (2017). PELI1 functions as a dual modulator of necroptosis and apoptosis by regulating ubiquitination of RIPK1 and mRNA levels of c-FLIP. Proc. Natl. Acad. Sci. USA *114*, 11944–11949.

Welz, P.S., Wullaert, A., Vlantis, K., Kondylis, V., Fernández-Majada, V., Ermolaeva, M., Kirsch, P., Sterner-Kock, A., van Loo, G., and Pasparakis, M. (2011). FADD prevents RIP3-mediated epithelial cell necrosis and chronic intestinal inflammation. Nature *477*, 330–334.

Xiao, Y., Jin, J., Chang, M., Chang, J.H., Hu, H., Zhou, X., Brittain, G.C., Stansberg, C., Torkildsen, Ø., Wang, X., et al. (2013). Peli1 promotes

microglia-mediated CNS inflammation by regulating Traf3 degradation. Nat. Med. *19*, 595–602.

Xie, T., Peng, W., Yan, C., Wu, J., Gong, X., and Shi, Y. (2013). Structural insights into RIP3-mediated necroptotic signaling. Cell Rep. *5*, 70–78.

Yang, X.D., and Sun, S.C. (2015). Targeting signaling factors for degradation, an emerging mechanism for TRAF functions. Immunol. Rev. *266*, 56–71.

Yatim, N., Jusforgues-Saklani, H., Orozco, S., Schulz, O., Barreira da Silva, R., Reis e Sousa, C., Green, D.R., Oberst, A., Albert, M.L., and Albert, M.L. (2015). RIPK1 and NF-κB signaling in dying cells determines cross-priming of $CD8^+$ T cells. Science *350*, 328–334.

Ye, Y., and Rape, M. (2009). Building ubiquitin chains: E2 enzymes at work. Nat. Rev. Mol. Cell Biol. *10*, 755–764.

Zhang, D.-W., Zheng, M., Zhao, J., Li, Y.-Y., Huang, Z., Li, Z., and Han, J. (2011). Multiple death pathways in TNF-treated fibroblasts: RIP3- and RIP1-dependent and independent routes. Cell Res. *21*, 368–371.

## STAR★METHODS

### KEY RESOURCES TABLE

| REAGENT or RESOURCE | SOURCE | IDENTIFIER |
|---|---|---|
| Antibodies | | |
| Anti-GFP (B-2) | Santa Cruz Biotechnology | sc-9996 |
| Anti-c-Myc (9E10) | Santa Cruz Biotechnology | sc-40 |
| Anti-HA-probe (F-7) | Santa Cruz Biotechnology | sc-7392 |
| Anti-Pellino 1/2 (F-7) | Santa Cruz Biotechnology | sc-271065 |
| Anti-Pellino 1 | Abcam | ab199336 |
| Anti-Ub (P4D1) | Santa Cruz Biotechnology | sc-8017 |
| Anti-FLAG | Sigma-Aldrich | F3165 |
| Anti-Actin | Sigma-Aldrich | A 3853 |
| Anti-LC3B | Sigma-Aldrich | L7543 |
| Anti-NIK | Cell Signaling Technology | 4994 |
| Anti-RIP1 | BD Transduction Laboratories | 610458 |
| Anti-RIP3 | Abcam | ab72106 |
| Anti-RIP3 | Enzo | ADI-905-242 |
| Anti-RIP3 | Bio-Rad Laboratories | AHP1797 |
| Anti-RIP3 | Cell Signaling Technology | 13526s |
| Anti-RIP3 (phospho S227) [EPR9627] | Abcam | ab209384 |
| Anti-MLKL (phospho S358) [EPR9514] | Abcam | ab187091 |
| Anti-MLKL (phospho S345) | Abcam | ab 196436 |
| Anti-Phospho-RIP1 (Ser166) | Cell Signaling Technology | 31122 |
| Anti-Phospho-RIP1 (Ser166) (D1L3S) | Cell Signaling Technology | 65746 |
| Anti-Phospho-RIP3 (Thr182) for human RIP3 | Abiocode, Inc | N/A |
| Anti-Ubiquitin | DAKO | Z0458 |
| Anti-Rabbit IgG (H+L) Secondary | Jackson Immuno Research Laboratories | 111-035-003 |
| Anti-Mouse IgG (H+L) Secondary | Jackson Immuno Research Laboratories | 515-035-003 |
| Anti-Rabbit IgG HRP | Rockland | 18-8816-33 |
| Anti-Mouse Ig HRP | Rockland | 18-8817-33 |
| Bacterial and Virus Strains | | |
| DH10Bac | Invitrogen | 10631-012 |
| DH5alpha | Real-Biotech Corporation | RH617 |
| Biological Samples | | |
| Skin biopsy specimens (TEN patients & normal tissues) | Ajou University Hospital | N/A |
| Chemicals, Peptides, and Recombinant Proteins | | |
| TNF-α | R&D Systems | 410-MT |
| zVAD | R&D Systems | FMK001 |
| SMAC mimetic (LCL-161) | Adooq Bioscience | A11928 |
| E64d | Sigma-Aldrich | E8640 |
| Bortezomib | Merck | 504313 |
| Cycloheximide | Calbiochem | 239764 |
| Chloroquine diphosphate (CQ) | Sigma-Aldrich | C6628 |
| Pepstatin A | Calbiochem | 516481 |
| MG132 | Calbiochem | 474790 |

(*Continued on next page*)

*Continued*

| REAGENT or RESOURCE | SOURCE | IDENTIFIER |
|---|---|---|
| Dabrafenib | Selleckchem | S2807 |
| Necrostatin-1 | Sigma-Aldrich | N9037 |
| Polyethylenimine | Polysciences | 23966-1 |
| Lipofectamine plus | Invitrogen | 11514-015 |
| Lipofectamine 2000 | Invitrogen | 11668-019 |
| TRIzol | Invitrogen | 15596-026 |
| amfiRivert cDNA Synthsis Platinum Master Mix | GenDEPOT | R5600-050 |
| enhanced chemiluminescence | Amersham | RPN2109 |
| GST-Ubiquitin E1 Enzyme(UBE1) | Boston biochem | E-306 |
| UbcH2/UBE2H | Boston biochem | E2-607 |
| $His_6$-UbcH3/Cdc34 | Boston biochem | E2-610 |
| UbcH5a/UBE2D1 | Boston biochem | E2-616 |
| UbcH5b/UBE2D2 | Boston biochem | E2-622 |
| UbcH5c/UBE2D3 | Boston biochem | E2-627 |
| $His_6$-UbcH6/UBE2E1 | Boston biochem | E2-630 |
| UbcH7/UBE2L3 | Boston biochem | E2-640 |
| $His_6$-UbcH10/UBE2C | Boston biochem | E2-650 |
| GST-UbcH12 | Boston biochem | E2-655 |
| $His_6$-UBE2N(Ubc13)/UBE2V1(Uev1) Complex | Boston biochem | E2-664 |
| $His_6$-Ubiquitin | Boston biochem | U-530 |
| Active human RIP3 full-length protein | Abcam | Ab125566 |
| Recombinant protein: RIP3(2-328bp) WT | This Paper | N/A |
| Recombinant protein: RIP3(2-328bp) K50A | This Paper | N/A |
| Recombinant protein: RIP3(2-328bp) T182A | This Paper | N/A |
| Recombinant protein: RIP3(2-328bp) S227A | This Paper | N/A |
| Recombinant protein: RIP3(2-328bp) T182A/S227A | This Paper | N/A |
| Recombinant protein: PELI1 WT | This Paper | N/A |
| Recombinant protein: PELI1 H313A | This Paper | N/A |
| Critical Commercial Assays | | |
| Site-directed mutagenesis kit | iNtRON biotechnology | 15071 |
| CellTiter-Glo Luminescent Cell Viability Assay kit | Promega | G7570 |
| CyroTox96 Non-Radioactive Cytotoxicity Assay | Promega | G1781 |
| Deposited Data | | |
| Immunoblot images | Mendeley Data | https://doi.org/10.17632/h8w33b7cpw.1 |
| Experimental Models: Cell Lines | | |
| Human: 293T | ATCC | CRL-3216 |
| Human: HeLa | ATCC | CCL-2 |
| Human: HT-29 | ATCC | HTB-38 |
| Human: H2009 | ATCC | CRL-5911 |
| Human: Raji | ATCC | CCL-86 |
| Human neonatal epidermal keratinocyte (HEKn) | GIBCO | C0015C |
| PELI1 WT MEF | This paper | N/A |
| PELI1 KO MEF | This paper | N/A |
| Insect cell line: Sf9 | ATCC | CRL-1711 |
| Oligonucleotides | | |
| Oligonucleotide list, see Primer Sequences Used in PCR below | This Paper | N/A |
| siRNA Non-target sequence: siNC | Bioneer | N/A |

(*Continued on next page*)

*Continued*

| REAGENT or RESOURCE | SOURCE | IDENTIFIER |
|---|---|---|
| siRNA targeting sequence: siPELI1 no. 1: CACACU AGCAUUUCCUAGU | Bioneer | N/A |
| siRNA targeting sequence: siPELI1 no. 2: GUGUUG UAUUUGUUCUAGU | Bioneer | N/A |
| PELI1 shRNA | Sigma-Aldrich | 0000420488 |
| PELI1 shRNA | Sigma-Aldrich | 0000430893 |
| Recombinant DNA | | |
| Plasmid: Flag-Ubiquitin WT | This Paper | N/A |
| Plasmid: Flag-Ubiquitin K48 only | This Paper | N/A |
| Plasmid: Flag-Ubiquitin K63 only | This Paper | N/A |
| Plasmid: HA-Ubiquitin WT | This Paper | N/A |
| Plasmid: GFP-PELI1 WT | This Paper | N/A |
| Plasmid: GFP-PELI1 H313A | This Paper | N/A |
| Plasmid: GFP-PELI1 C336A | This Paper | N/A |
| Plasmid: GFP-PELI1 R104A | This Paper | N/A |
| Plasmid: Myc-PELI1 WT | This Paper | N/A |
| Plasmid: Myc-PELI1 C-term deletion | This Paper | N/A |
| Plasmid: Myc-CHIP | This Paper | N/A |
| Plasmid: GFP-BUB1B | This Paper | N/A |
| Plasmid: GFP-TRAF2 | This Paper | N/A |
| Plasmid: Myc-RIP1 | This Paper | N/A |
| Plasmid: Flag-IRAK1 | This Paper | N/A |
| Plasmid: Flag-RIP3 | This Paper | N/A |
| Plasmid: Flag-mouse RIP3 | This Paper | N/A |
| Plasmid: Flag-RIP3 K5A | This Paper | N/A |
| Plasmid: Flag-RIP3 K50A | This Paper | N/A |
| Plasmid: Flag-RIP3 T182S | This Paper | N/A |
| Plasmid: Flag-RIP3 T182A | This Paper | N/A |
| Plasmid: Flag-RIP3 Y185A | This Paper | N/A |
| Plasmid: Flag-RIP3 Y185F | This Paper | N/A |
| Plasmid: Flag-RIP3 T200A | This Paper | N/A |
| Plasmid: Flag-RIP3 T224A | This Paper | N/A |
| Plasmid: Flag-RIP3 S227A | This Paper | N/A |
| Plasmid: Flag-RIP3 S227D | This Paper | N/A |
| Plasmid: Flag-RIP3 K259R | This Paper | N/A |
| Plasmid: Flag-RIP3 T300A | This Paper | N/A |
| Plasmid: Flag-RIP3 T325A | This Paper | N/A |
| Plasmid: Flag-RIP3 K351R | This Paper | N/A |
| Plasmid: Flag-RIP3 T369A | This Paper | N/A |
| Plasmid: Flag-RIP3 T387A | This Paper | N/A |
| Plasmid: Flag-RIP3 K501R | This Paper | N/A |
| Plasmid: pLX303/HA-3XFlag-RIP3 | This Paper | N/A |
| Plasmid: pLX 303/HA-3XFlag-RIP3 T182A | This Paper | N/A |
| Software and Algorithms | | |
| MEGA6 | Molecular Evolutionary Genetics Analysis | https://www.megasoftware.net/ |
| Cytoscape | Cytoscape Consortium | http://www.cytoscape.org |
| PyMOL | PyMOL | https://www.pymol.org/2 |

(*Continued on next page*)

*Continued*

| REAGENT or RESOURCE | SOURCE | IDENTIFIER |
|---|---|---|
| Image Pro Plus, Version 4.5 | Media Cybertics Co., Silver Spring, MD, USA | http://www.mediacy.com/imageproplus |
| GenePix® Pro 7 Software | Molecular Devices | https://www.moleculardevices.com/en/asset/br/data-sheets/genepix-pro-software-datasheet-v7-rev-b |
| Other | | |
| GenePix 4000B Microarray Scanner | Axon Instruments | N/A |
| Human Proteome Microarray v2.0 | CDI Laboratories Inc. | N/A |

## CONTACT FOR REAGENT AND RESOURCE SHARING

As Lead Contact, You-Sun Kim is responsible for all reagent and resource requests. Please contact You-Sun Kim at yousunkim@ajou.ac.kr with requests and inquiries.

## METHOD DETAILS

### Cell lines and culture conditions

HEK293T, HeLa, and HT-29 cells were grown in Dulbecco's Modified Eagle's Medium (DMEM) supplemented with 10% fetal bovine serum (FBS). H2009 and Raji cells were maintained in Roswell Park Memorial Institute (RPMI) 1640 supplemented with 10% FBS. WT and PELI1−/− mouse embryonic fibroblast (MEF) cells were generated from two different PELI1 knockout mice, and their culture conditions have been previously described (Chang et al., 2009; Kim et al., 2017). To generate cell lines stably expressing RIP3 construct, HeLa cells were infected with pLX303-hRIP3 lentivirus. To generate stable knockdown cell line of PELI1 expression, HT-29 and RIP3 (stable ectopic)-expressing HeLa cells were infected with PELI1 shRNA lentivirus and selected for puromycin resistance. Human neonatal epidermal keratinocytes (HEKn) were from GIBCO and maintained according to the manufacturer's instructions in Epilife medium with human keratinocytes growth supplement. Cells at passage 3-6 were used for experiments.

### Antibodies and chemical reagents

Antibodies used for immunoblot and immunoprecipitation analysis were as follows: anti-GFP (Santa Cruz, sc-9996, 1:1000 dilution), anti-Myc (Santa Cruz, sc-40, 1:1000), anti-HA (Santa Cruz, sc-7392, 1:1000), anti-GAPDH (Santa Cruz, sc-25778, 1:2500), anti-Pellino1 (Santa Cruz, sc-271065, 1:1000), anti-ubiquitin (Santa Cruz, sc-8017, 1:1000), anti-Flag (Sigma, F3165, 1:1000), anti-actin (Sigma, A 3853, 1:2500) and LC3 (Sigma, L7543, 1:2500), anti-NIK (CST, no. 4994, 1:1000), anti-RIP1 (BD, no. 610458, 1:1000), anti-RIP3 (Abcam, ab72106, 1:1000), anti-p-RIP3 (S227) (Abcam, ab209384, 1:5000), anti-p-MLKL (Abcam, ab187091, 1:1000). The phospho-specific antibody against pT182 of human RIP3 was generated by Abiocode, Inc. TNF-$\alpha$ and zVAD were purchased from R&D Systems. SMAC mimetic (LCL-161) was from Adooq Bioscience. E64d and chloroquine diphosphate (CQ)were from Sigma-Aldrich. Cycloheximide, pepstatin A, and MG132 were from Calbiochem. Dabrafenib was from Selleckchem. Bortezomib was from Merck.

### Plasmid construction, mutagenesis, and transfection

Flag-tagged WT, K48 only-, or K63-only ubiquitin constructs and WT, R104A, H313A, and C336A mutants for GFP-tagged PELI1 constructs encoding human PELI1 were kindly provided by Dr. H.C. Kang (Ajou University, Suwon, Korea). Myc-tagged PELI1 WT and the C-terminal deletion mutant were from Dr. C.W. Lee (Sungkyunkwan University, Suwon, Korea). Dr. J.Y. Cho (Sungkyunkwan University, Suwon, Korea) kindly provided the Flag-tagged IRAK1 expression plasmid. Various RIP3 and PELI1 mutants were generated by the site-directed mutagenesis kit (iNtRON biotechnology, Korea) according to the manufacturer's instructions and subjected to DNA sequencing for verification. PCRs were performed with the oligonucleotide list below. For a transient ectopic expression, expression constructs were transfected into cells using either polyethylenimine (Polysciences) or Lipofectamine plus (Invitrogen), according to the manufacturer's instructions. An empty vector, pcDNA3, was used to adjust total DNA amount where necessary. For *in vivo* ubiquitylation asssay, HA or Flag-tagged ubiquitin construct was used.

| Primer Sequences Used in PCR | | |
|---|---|---|
| Target | Sense (5′-3′) | Anti-sense (5′-3′) |
| Actin | CAGGTCATCACCATTGGCAATGAGC | GATGTCCACGTCACACTTCATGA |
| RIP3-WT | CAAGGAGGGACAGAAATGGA | GCCTTCTTGCGAACCTACTG |
| RIP3-T182A | CGGGGAGCCAGGGGGC GCCCTGGGCTACTTGGCCC | GGGCCAAGTAGCCCAGGG CGCCCCCTGGCTCCCCG |
| RIP3-T200A | AAACCGGAAGGCCTCCGCA GCCAGTGACGTCTACA | TGTAGACGTCACTGGCTG CGGAGGCCTTCCGGTTT |
| RIP3-T224A | AGAAGTTGAGTTGCCAGC CGAACCATCACTCGTGT | ACACGAGTGATGGTTCG GCTGGCAACTCAACTTCT |
| RIP3-T300A | GAATGCTGCTGTCTCCGC GGTAAAGGATTTCCTGT | ACAGGAAATCCTTTACCGC GGAGACAGCAGCATTC |
| RIP3-T325A | GTCAGGCCAAGGAGGGGC AGAAATGGATGGCTTTA | TAAAGCCATCCATTTCTGC CCCTCCTTGGCCTGAC |
| RIP3-T369A | AAAATGCCCGAGCCTTGC CAAGAGGAGCAGGGCAC | GTGCCCTGCTCCTCTTG GCAAGGCTCGGGCATTTT |
| RIP3-T387A | AGCCTGGACAGCAGGCGC ATCTTCAGATTCGATGG | CCATCGAATCTGAAGATG CGCCTGCTGTCCAGGCT |
| RIP3-K5A | ATGTCGTGCGTCGCGTTAT GGCCCAGCGGTGCCCC | GGGGCACCGCTGGGCCATA ACGCGACGCACGACAT |
| RIP3-K50A | CTACGATGTGGCGGTCGCG ATCGTAAACTCAAAGG | CCTTTGAGTTTACGATCG CGACCGCCACATCGTAG |
| RIP3-K259R | CGGCTTAGAAGGACTGAGG GAGCTAATGCAGCTC | AGAGCTGCATTAGCTCCCT CAGTCCTTCTAAGCCG |
| RIP3-K351R | TTCTGAGTGGCTAAACAGA CTGAATCTAGAGGAGC | GCTCCTCTAGATTCAGTC TGTTTAGCCACTCAGAA |
| RIP3-K363R | TCCCAGCTCTGTTCCTCGA AAATGCCCGAGCCTTA | TAAGGCTCGGGCATTTTC GAGGAACAGAGCTGGGA |
| RIP3-K501R | TTCGCAAGAAGGCCCTAGA GATCCTGAAGCCTGGA | TCCAGGCTTCAGGATCTC TAGGGCCTTCTTGCGAA |
| RIP3-T182D | CGGGGAGCCAGGGGGCG ACCTGGGCTACTTGGCCC | GGGCCAAGTAGCCCAGGTC GCCCCCTGGCTCCCCG |
| RIP3-T182E | CGGGGAGCCAGGGGGCGA ACTGGGCTACTTGGCCC | GGGCCAAGTAGCCCAGTTC GCCCCCTGGCTCCCCG |
| RIP3-T182S | CGGGGAGCCAGGGGGCGA CCTGGGCTACTTGGCCC | GGGCCAAGTAGCCCAGGG AGCCCCCTGGCTCCCCG |
| RIP3-S227A | GTTGCCAACCGAACCAGCA CTCGTGTACGAAGCAG | CTGCTTCGTACACGAGT GCTGGTTCGGTTGGCAAC |
| RIP3-S227D | GTTGCCAACCGAACCAAG ACTCGTGTACGAAGCAG | CTGCTTCGTACACGAGT CTTGGTTCGGTTGGCAAC |
| PELI1-WT | AGATGGATGGCTTGACCACT | TGCTGCATTGATTTCCTGTC |
| PELI1-R104A | TATGTTTCAGATTGGCGC GTCGACTGAAAGCCCCA | TGGGGCTTTCAGTCGAC GCGCCAATCTGAAACATA |

### siRNA, shRNA, and reverse transcription-PCR (RT-PCR)

Double-stranded small interfering RNAs (siRNA) for human PELI1 and control siRNA were purchased from Bioneer and were transfected using Lipofectamine 2000 (Invitrogen). The siRNA sequences for PELI1 are as follows: siPELI1 no. 1, 5′-CACACUAGCAUUUC CUAGU-3′; no. 2, 5′-GUGUUGUAUUUGUUCUAGU-3′. The PELI1 short hairpin RNA (shRNA) lentiviral construct was purchased from Sigma, and lentiviral particle for PELI1 shRNA was prepared as previously described (Koo et al., 2015). Total RNA was isolated from indicated cell lines using the TRIzol reagent (Life Technologies), according to the manufacturer's instructions. The concentration and purity of the RNA samples were measured with a NanoDrop (Thermo Scientific), with $A_{260/280}$ ratios ranging from 1.8 to 2.0 considered acceptable. The amfiRivert cDNA Synthsis Platinum Master Mix (GenDEPOT) was used for cDNA synthesis. PCR was performed with the oligonucleotides listed in the table above.

### Cytotoxicity Assays

Cell viability was determined using tetrazolium dye colorimetric tests (MTT assay) read at 570 nm. Lactate dehydrogenase (LDH) leakage was quantified using the CellTiter-Glo Luminescent Cell Viability Assay kit (Promega, G7570) according to the manufacturer's instructions. LDH absorbance was read at 490 nm. Luminescence was measured using a POLARstar OPTIMA. For CellTiter-Glo assays, the mean ± STDEV of duplicates is presented.

### Immunoprecipitation and immunoblot analysis

Cells lysis was in M2 buffer (Kim et al., 2007). Equal amounts of cell extracts were resolved by SDS-PAGE and analyzed by immunoblotting. For immunoprecipitation, lysates were mixed and precipitated with antibody and protein A-Sepharose or protein G-agarose beads overnight or 3 hr at 4°C. Bound proteins were removed by boiling in SDS and resolved by SDS-PAGE and immunoblotting visualized by enhanced chemiluminescence (ECL, Amersham).

### *In vitro* ubiquitylation assay

To measure auto-ubiquitylation activity of PELI1, E1 (50 nM), UbcHs (50 nM), and recombinant PELI1 (1 μg/μL) were incubated with ubiquitin (200 mM) at 37°C in the ubiquitylation buffer containing 50 mM Tris-Cl, pH 7.5, 2.5 mM $MgCl_2$, 2 mM DTT, 2 mM ATP. For reducing conditions, samples were treated with Laemmli sample buffer (Bio-Rad) and boiled supernatants were separated by 4%–20% gradient SDS-PAGE. Auto-ubiquitylated PELI1 was detected by immunoblot with anti-ubiquitin antibody. For the *in vitro* RIP3 ubiquitylation assay, recombinant RIP3 (1 μg/μL) was incubated with E1 (50 nM), UbcH5c (50 nM), and recombinant PELI1 (1 μg/μL) in the ubiquitylation buffer for 1 hr at 37°C. To detect PELI1-mediated RIP3 ubiquitylation, samples were loaded into 4%–20% gradient SDS-PAGE and then immunoblotted. All proteins loaded in SDS-PAGE were separately visualized by Coomassie staining. Recombinant E1, UbcHs and ubiquitin were purchased from Boston Biochem.

### Protein Microarray

The protein microarray experiment was performed by using a HuProt human proteome microarray v2.0 (CDI Laboratories). The protein chip was equilibrated with microarray buffer containing (137 mM NaCl, 2.7 mM KCl, 4.3 mM $Na_2HPO_4$, 1.47 mM $KH_2PO_4$, pH 7.4, 0.1% Triton X-100) for 5 min at RT and sequentially incubated with blocking solution composed of 5% filtrated dry milk in microarray buffer for 1 hr at RT. For screening of RIP3 binding proteins, a blocked protein chip was washed 3 times with microarray buffer for 10 min, followed by incubation with RIP3 recombinant proteins (Abcam) at a dilution of 2 μg/mL for 8 hr at 4°C. To apply RIP3 antibody on the protein chip, residual non-bound RIP3 proteins were removed by washing with microarray buffer for 10 min. A washed protein chip was incubated with polyclonal anti-RIP3 (1:1000) in microarray buffer containing 1% filtrated dry milk for 2 hr and then followed by washing 3 times. Sequentially, secondary anti-rabbit Alex-fluor 647 (1:5000) was incubated for 1 hr at RT and then washed 3 times with microarray buffer. The protein chip was dried via centrifugation at 200 *g* for 2 min using a 50 mL conical tube and then scanned with GenePix 4000B (Axon Instruments, Union City, CA). Following scanning, the signal intensity value for each spot was obtained as the ratio of foreground to background signals and normalized with GST signal intensity. The mean of signal intensity of all proteins on the chip was calculated.

### Mass Spectrometric Analysis

Following the *in vitro* RIP3 ubiquitylation assay, ubiquitylated RIP3 bands were excised and sequenced by mass spectrometry.

### RIP3 structure modeling

A molecular model of human RIP3 was generated using the structure of mouse RIP3 in complex with MLKL (PDB: 4M69) as a template (Xie et al., 2013). The initial model was energy-minimized with SPBDV (Guex et al., 2009). Structural analysis and display were performed using PyMOL (https://www.pymol.org/2).

### Purification of recombinant proteins

For purifying recombinant RIP3 protein derived from insect cells, DH10Bac *E. coli* were transfected with pDEST20 to generate recombinant bacmid DNA. Sf9 cells were then transfected with purified bacmid DNA. The protein expression was tested by immunoblotting with anti-GST antibody. For protein expression, Sf9 cells were infected with baculovirus and after 5 days later, cells were collected and lyzed with NETN buffer (25 mM Tris-HCl pH 8.0, 150 mM NaCl, 1 mM DTT, 1% NP-40, 0.1% Triton X-100 and protease inhibitor). The soluble fraction was separated by centrifugation and incubated with glutathione Sepharose 4B beads at 4°C for 3 hr. The protein-bound beads were washed with NETN buffer and eluted with elution buffer (50 mM HEPES pH 7.5, 100 mM NaCl, 30% glycerol, 40 mM L-glutathione reduced, and 0.03% Triton X-100).

### *In vitro* kinase assays

Purified baculovirus-expressed recombinant human RIP3 kinase domain (amino acids [aa] 2-328) from WT and mutant constructs were incubated with kinase buffer and [$\gamma$-$^{32}$P]ATP for 30 min at 30°C. After incubation, samples were boiled and resolved by SDS-PAGE. Kinase activity was determined by radiography. Recombinant proteins were also incubated with kinase buffer and cold ATP for 30 min at 30°C. After incubation, samples were boiled and resolved by SDS-PAGE. The kinase activity for S227

auto-phosphorylation was determined by western blotting with specific phospho-S227 antibody. 293T cells were transfected with different Flag-tagged RIP3 or mutants and at 24 hr post-transfection, cells were lysed in M2 buffer. The lysates were incubated with Flag-tagged beads overnight and the immune complexes were washed four times and re-suspended in kinase buffer followed by addition of [$\gamma$-$^{32}$P] ATP for 30 min at 30°C. After incubation, samples were boiled and resolved by SDS-PAGE. Kinase activity was determined by autoradiography.

### Immunohistochemistry and Image analysis

Punch skin biopsy specimens (3 mm) were taken from 6 TEN patients. Five normal tissues from patients who had done skin biopsies for diagnosis of pigmentary disease were used as controls. Paraffin-embedded tissue sections of 3-$\mu$m thickness were processed for light microscopic examination. Immunohistochemistry was performed using standard techniques using primary antibodies to RIP3 and PELI1. Quantitative analysis of immunohistochemical stains was done using Image Pro Plus, Version 4.5; (Media Cybertics Co., Silver Spring, MD, USA), performed on a representative area of each specimen. The ratio of stained area to the measured epidermal area (Pigmented Area per measured Epidermal Area, PA/EA) was measured in TEN skin lesions and normal skin.

## DATA AND SOFTWARE AVAILABILITY

Images for all immunoblots have been deposited to Mendeley Data: https://doi.org/10.17632/h8w33b7cpw.1.

## QUANTIFICATION AND STATISTICAL ANALYSIS

Each experiment was repeated three times or more. Statistical analysis was performed using ANOVA and an unpaired Student's t test. Data are presented as means ± SEM. P value < 0.01 was considered statistically significant.